ChemPubSoc Europe

DOI: 10.1002/chem.201303841

CHEMISTRY A European Journal Full Paper

Macrocyclic Peptides

Synthesis and Conformational Analysis of Cyclic Homooligomers from Pyranoid ε-Sugar Amino Acids

Andrés Feher-Voelger,[a] Jorge Borges-González,[a] Romen Carrillo,[a] Ezequiel Q. Morales,[a] Javier González-Platas,[b] and Tomás Martín*[a, c]

Dedicated to Professor Victor S. Martín on the occasion of his 60th birthday

Abstract: New pyranoid ε-sugar amino acids were designed as building blocks, in which the carboxylic acid and the amine groups were placed in positions C2 and C3 with respect to the tetrahydropyran oxygen atom. By using standard solution-phase coupling procedures, cyclic homooligomers containing pyranoid ε-sugar amino acids were synthesized. Conformation analysis was performed by using NMR spectroscopic experiments, FTIR spectroscopic studies, X-ray analysis, and a theoretical conformation search. These studies reveal that the presence of a methoxy group in the position C4 of the pyran ring produces an important structural change in the cyclodipeptides. When the methoxy groups are present, the structure collapses through interresidue hydrogen bonds between the oxygen atoms of the pyran ring and the amide protons. However, when the cyclodipeptide lacks the methoxy groups, a U-shape structure is adopted, in which there is a hydrophilic concave face with four oxygen atoms and two amide protons directed toward the center of the cavity. Additionally, we found important evidence of the key role played by weak electrostatic interactions, such as the five-membered hydrogen-bonded pseudocycles (C_5) between the amide protons and the ether oxygen atoms, in the conformation equilibrium of the macrocycles and in the cyclization step of the cyclic tetrapeptides.

Introduction

In the last few years, macrocyclic peptides have attracted considerable attention as potential scaffolds in medicinal chemistry for the development of new drugs.[1] Cyclization of the linear precursors provides, on one hand, a valuable tool to introduce steric and angular constraints into the macrocycles, which restrict their conformational degrees of freedom and potentially can impart higher target binding and selectivity; on the other hand, cyclization also improves the resistance to proteolytic degradation and oral bioavailability.[2] A large number of natural and synthetic cyclic peptides have been reported to display remarkable biological activity, such as cyclosporine A,[3] antamanide,[2] microcystin LR,[4] octapeptidic somatostatin analogues,[5] and so forth. All those peptides, and actually any potential drug to be evaluated, must be not only bioactive, but also bioavailable, and therefore these drugs must reach the therapeutic target once introduced into a living organism, which usually implies going through the cellular membrane. In fact, all the above-mentioned cyclic peptides display a good absorption through the gastrointestinal tract. However, oddly enough, the "rule of five" stated by Lipinski et al. [6] states that most of the cyclic peptides should not be able to cross the membrane due to a high number of hydrogen-bond donors and acceptors and low theoretical octanol/water (o/w) partition coefficients ($C\log P_{o/w}$). This outcome should result in a very low passive permeability (transcellular pathway) of the cyclic peptides through the cellular membrane, and therefore a scarce bioavailability. This apparent contradiction between the Lipinski rules and experimental outcomes is due to particular three-dimensional arrangements of the cyclic peptides. In general, cyclic peptides are not rigid compounds; instead, they have a compromise between preorganization and structural flexibility, which can increase membrane permeability providing that there are conformations that maximize the internal hydrogen bonds (folded conformers).[7] In this way, in nonpolar environments, the polar groups interact with each other to form internal backbone hydrogen bonds and the nonpolar

[a] Dr. A. Feher-Voelger, J. Borges-González, Dr. R. Carrillo, Dr. E. Q. Morales, Dr. T. Martín
Instituto de Productos Naturales y Agrobiología-CSIC
Avda. Astrofísico Francisco Sánchez, 3
38206-La Laguna, Tenerife (Spain)
Fax: (+34) 922-260135
E-mail: tmartin@ipna.csic.es

[b] Dr. J. González-Platas
Servicio de Difracción de Rayos X
Departamento de Física Fundamental II, Universidad de La Laguna
Avda. Astrofísico Francisco Sánchez, 2
38206-La Laguna, Tenerife (Spain)

[c] Dr. T. Martín
Instituto Universitario de Bio-Orgánica "Antonio González"
Avda. Astrofísico Francisco Sánchez, 2
38206-La Laguna, Tenerife (Spain)

Supporting information for this article is available on the WWW under http://dx.doi.org/10.1002/chem.201303841.

groups would be pointing outward. In this regard, recent studies show that solvent shielding of the amide bonds by N-methylation plays an important role in imparting permeability to the cyclic peptides.[5,8] However, it is quite difficult to predict the impact of N-methylation on the conformation equilibrium of cyclic peptides. Therefore, the search for new strategies in the conformational control of cyclic peptides is of significant interest. The development of suitable models to understand and modulate the formation of an internal network of hydrogen bonds is vital to understand the passive permeability of cyclic peptides better and to develop future smart applications of such an exciting prospect.

With this aim in mind, sugar amino acid units (SAAs) were considered as an optimal choice for the synthesis of model cyclic peptide homooligomers to study if weak noncovalent interactions can modulate the internal backbone of hydrogen bonds. SAAs are hybrid scaffolds that combine elements from carbohydrates and amino acids in their structure. There are several advantageous features displayed by SAAs concerning our above-mentioned purpose, among which it is worth mentioning a controllable and partially predictable conformational restriction and the ability of SAAs to modulate chemical functionality and stereochemistry precisely. Since these compounds were first employed as useful peptide building blocks, diverse types of furanoid[9] and pyranoid[10] α-, β-, γ-, and δ-SAAs have been described as conformationally constrained scaffolds for the formation of cyclic peptides.[11]

Previous studies in our group have shown that some derivatives of the *cis*-2-oxymethyl-3-oxytetrahydropyran unit, although quite flexible, display inherent conformational preferences.[12] Particularly interesting are some macrooligolides made from such a scaffold, modified to display an ε-hydroxy acid unit.[13] Thus, it is reasonable to base the design of our model cyclic peptide homooligomers on a ε-SAA unit by simply changing the hydroxy group for an amine group. Curiously, there are scarce precedents that use ε-SAAs in cyclic homooligomers,[14] and in all these cases the amine and carboxylic acid groups were linked through the adjacent positions to the oxygen atom in such a way that the oxygen atom of the ring is part of the macrocycle. In our case, the carboxylic acid and amine groups are placed at C2 and C3, thus leaving the tetrahydropyran oxygen atom in a suitable position to act as a weak hydrogen-bond acceptor, which can have a modulating effect over other noncovalent interactions (Figure 1). Moreover, the carboxylic acid and sugar moieties are linked through an ether group, the oxygen atom of which might participate in a five-membered hydrogen-bonded pseudocyclic (C_5) interaction, with the NH of the amide group helping to create an internal backbone of hydrogen bonds in the cyclic peptides.[15] Finally, we introduce a methoxy group at C4 as an additional appendix, which can act as a control element of the conformation equilibrium (Figure 1). Taking all these design features into account, we describe herein the synthesis of cyclic homooligomers from pyranoid ε-SAAs analogues. Additionally, a detailed conformation analysis was made both in solution and the solid state to understand and measure the effect of all the above-mentioned conformational control factors.

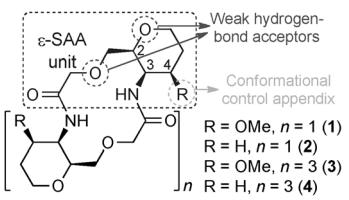

Figure 1. Structures of the cyclic peptides designed based on ε-SAA units.

Results and Discussion

Synthesis

Usually the synthetic strategies to obtain cyclic peptides require the use of orthogonally protected amino acid units. Taking this approach into account, we chose *tert*-butyl ester and azide groups as precursors to the acid and amine groups, respectively. This strategy was previously described by Koert and co-workers.[15d] A commercially available starting material, tri-*O*-acetyl-D-glucal, was used as the common precursor for the synthesis of both analogues of the ε-SAA units, that is, compounds **5** and **6** (Scheme 1).

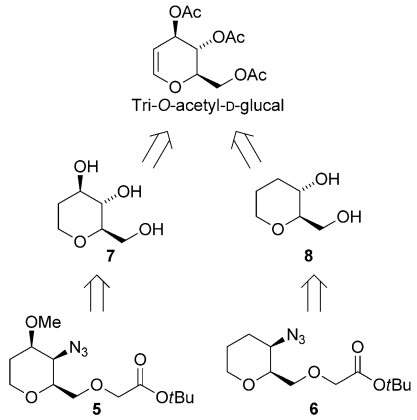

Scheme 1. Retrosynthetic analysis for the synthesis of analogues of the ε-SAA units **5** and **6**.

Tri-*O*-acetyl-D-glucal was converted into the corresponding triol **7**[16] and diol **8**[17] by using previously described procedures. The benzylidenation of triol **7** followed by methylation gave compound **9**.[18] With the first step, we achieved one important goal: the chemical differentiation between the two secondary hydroxy groups. With the benzylidenacetal **9** in hand, the next step was a regioselective reduction by using the BH_3·THF complex and a catalytic amount of $Cu(OTf)_2$ to afford the secondary benzyl ether,[19] which was submitted to *O*-alkylation of the primary alcohol with *tert*-butyl 2-bromoacetate to obtain the *tert*-butyl ester **10**.[20] Cleavage of the benzyl protecting group under hydrogenation conditions provided the secondary alcohol, which was used to obtain the masked ε-SAA unit **5** by using a Mitsunobu reaction with diphenyl-

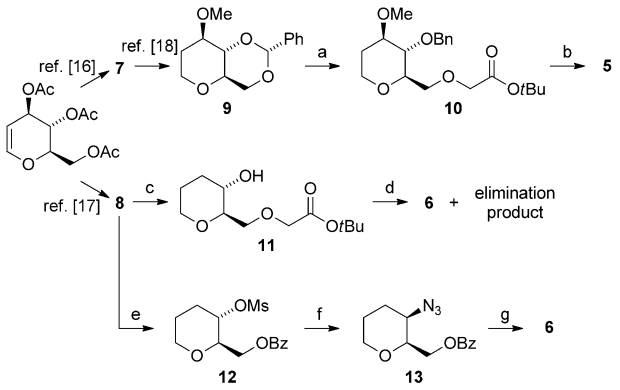

Scheme 2. Synthesis of the masked ε-SAA units **5** and **6**. Reagents and conditions: a) 1) BH_3·THF, $Cu(OTf)_2$, THF, RT (98%); 2) NaH, $BrCH_2CO_2tBu$, THF, RT (89%); b) 1) H_2, Pd(C), MeOH, RT; 2) DIAD, DPPA, PPh_3, THF (95% over 2 steps); c) NaH, $BrCH_2CO_2tBu$, THF, 0 °C (60%); d) DIAD, DPPA, PPh_3, THF (83%); e) 1) BzCl, Et_3N, CH_2Cl_2; 2) MsCl, Et_3N, CH_2Cl_2 (92% over 2 steps); f) NaN_3, DMF, 100 °C (85%); g) 1) K_2CO_3, MeOH; 2) NaH, $BrCH_2CO_2tBu$, THF, RT (75% over 2 steps). Bz = benzoyl, DIAD = diisopropyl azodicarboxylate, DPPA = diphenyl phosphorazidate, Ms = methanesulfonyl.

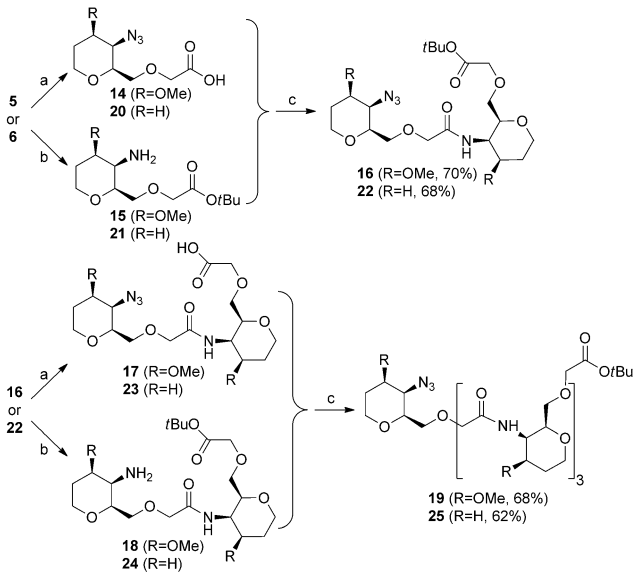

Scheme 3. Divergent–convergent synthesis of linear precursors **16** and **22** of the cyclic dipeptides and linear precursors **19** and **25** of the cyclic tetrapeptides. Reagents and conditions: a) TFA, CH_2Cl_2, RT; b) H_2, Pd(C), MeOH, RT; c) EDCI, HOBt, DIPEA, CH_2Cl_2, RT. DIPEA = *N*,*N*-diisopropylethylamine, EDCI = 1-ethyl-3-[3-(dimethylamino)propyl]carbodiimide hydrochloride, HOBt = 1-hydroxybenzotriazole.

phosphoryl azide (DPPA),[21] which introduced an azide group with complete inversion of the configuration (Scheme 2).

To carry out the synthesis of the masked ε-SAA unit **6**, a similar strategy was attempted. Thus, selective *O*-alkylation of the diol **8** with *tert*-butyl 2-bromoacetate was performed to afford alcohol **11** in moderate yield. Unfortunately, this approach failed because the Mitsunobu reaction provided an equimolar mixture of the desired compound **6** along with elimination product, which were difficult to separate.[22] As a result of this outcome, a new approach was developed for the synthesis of **6**. We selectively protected the primary alcohol of diol **8** as a benzoate group, and then the secondary alcohol was converted to give the mesylate compound **12**, which was transformed into azide **13** by nucleophile displacement with NaN_3. Finally, deprotection of the benzoate and further *O*-alkylation with *tert*-butyl 2-bromoacetate afforded the ε-SAA unit **6** in a good yield (Scheme 2).

The cyclic homooligomers were synthesized from their linear precursors through a head-to-tail cyclization. The linear dimers and tetramers were prepared by using conventional solution-phase peptide synthetic methods by means of a divergent–convergent strategy. Thus, with the protected monomer **5** in hand, acidic hydrolysis of the *tert*-butyl ester or hydrogenation of the azide group gave the primary coupling partners carboxylic acid **14** and amine **15**, respectively. Standard peptide-bond formation conditions by using EDCI with stoichiometric amounts of HOBt and DIPEA were employed, thus affording the pseudo-dipeptide **16** in good yield (Scheme 3). The pseudo-dipeptide **16** served as a common intermediate to prepare the carboxylic acid **17** and amine **18** required for the pseudotetrapeptide synthesis. A portion of **16** was converted into the free carboxylic dipeptide **17**, and the rest of **16** was converted into the unmasked dipeptide amine **18**. Finally, coupling of **17** and **18** by using the above-described procedure afforded the pseudo-tetrapeptide **19** in good yield. By using monomer **6** and applying the same sequence of reactions described above, the linear precursors **22** and **25** were obtained (Scheme 3).

At this point of the synthesis, hydrogenation of the azide group followed by acidic hydrolysis of the *tert*-butyl ester moiety of all the linear precursors **16**, **19**, **22**, and **25** yielded the corresponding amino acids **26**–**29**, respectively. Cyclization of **26** to the cyclic dipeptide **1** proceeded under high-dilution conditions (0.001 M) in CH_2Cl_2 with EDCI, HOBt, and DIPEA over a period of 72 hours. The reaction of amino acid **27** under the conditions described above furnished the cyclic tetrapeptide **3** in 43% yield (Scheme 4).

Macrolactamization of amino acid **28** worked better when HBTU was used as a coupling agent, thus affording the cyclic dipeptide **2** in moderate yield. Unfortunately, these experimental conditions failed when cyclization of amino acid **29** was performed. We also explored the use of different coupling agents (i.e., *N*,*N*-dicyclohexylcarbodiimide (DCC), EDCI, diethylphosphoryl cyanide (DEPC), and benzotriazol-1-yloxytris(dimethylamino)phosphonium hexafluorophosphate (BOP)) and different experimental conditions (i.e., temperature and high-dilution conditions in CH_2Cl_2, DMF, and a mixture of both); however, all these attempts failed (see below), and we were unable to obtain the cyclic tetrapeptide **4** (Scheme 4).

Conformational analysis

NMR and IR spectroscopic studies

The NMR spectra (^1H and ^{13}C) of all the cyclic peptides displayed symmetric structures with only one set of resonances from their constituent ε-SAA units in all the solvents in which

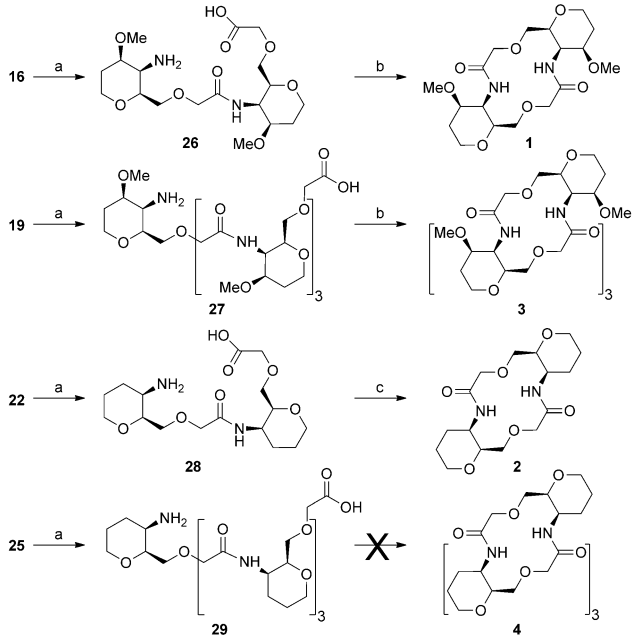

Scheme 4. Synthesis of cyclic dipeptides **1** and **2** and cyclic tetrapeptides **3** and **4**. Reagents and conditions: a) 1) H_2, Pd(C), MeOH, RT; 2) TFA, CH_2Cl_2, RT; b) EDCI, HOBt, DIPEA, CH_2Cl_2, RT (38 and 43% for **1** and **3**, respectively); c) HBTU, DIPEA, CH_2Cl_2, RT (31%). HBTU = *O*-(benzotriazol-1-yl)-*N*,*N*,*N*′,*N*′-tetramethyluronium hexafluorophosphate.

they were studied. The NMR spectra of the cyclic products **2** and **3** in C_6D_6 were better dispersed and resolved than in $CDCl_3$. Therefore, two-dimensional NMR spectroscopic experiments for the cyclic peptides **2** and **3** (i.e., COSY, HSQC, HMBC, and NOESY) were performed in C_6D_6, and most of the spectral parameters could be obtained and are reported in Table 1. However, cyclodipeptide **1** in $CDCl_3$ showed better resolution in the NMR spectra than in C_6D_6. Also, variable-temperature studies were carried out in $CDCl_3$ instead of C_6D_6 to increase the range of low temperatures. These experiments were used to measure the temperature coefficients ($\Delta\delta/\Delta T$) of the amide-proton chemical shifts, which were used to determine their implications in intramolecular hydrogen bonds. FTIR spectroscopic analysis was performed in CH_2Cl_2 to differentiate the hydrogen-bonded from the non-hydrogen-bonded amide groups, thus yielding further evidence of the presence of hydrogen-bonded conformations.

Conformational analysis of 1

The cyclic dimer **1** is a 14-membered macrocyclic peptide. The ^{1}H NMR spectrum of **1** recorded in $CDCl_3$, C_6D_6, [D_6]DMSO, and D_2O at 300 K showed a symmetrical set of high-resolution signals, which is consistent with the macrocycle either having a rigid conformation with C_2 symmetry or a structure involved in a fast conformation equilibrium. Chemical shifts of the amide proton in $CDCl_3$ (δ_{NH} = 7.65 ppm) remained constant as the sample concentration was diluted from 25 to 1.0 mM, which clearly suggested that N–H bonds are involved in intramolecular hydrogen bonds. Also, the amide proton displays a large coupling constant with a proton at C3 ($^3J_{NH-C3H}$ = 10.4 Hz), which corresponds to an antiperiplanar arrangement (H-*N*-C3–H ≈ 180°). COSY, HSQC, and NOESY experiments were performed at 300 K to assign all the signals. The NOESY spectrum shows several well-resolved cross-peaks, most of which are either intraresidue or sequential. Coupling constants and NOE interactions between protons of the pyranose rings confirmed a chair conformation with substituents at the C2 and C4 equatorial positions and a substituent at the C3 axial position. Diastereotopic assignment of the prochiral methylene protons at C7 was carried out on the basis of the $^3J_{2,7}$ coupling constants and NOE interactions. Thus, the coupling constant values were $^3J_{C2H-C7H proR}$ = 10.7 and $^3J_{C2H-C7H proS}$ = 4.6 in $CDCl_3$,

Table 1. ^{1}H NMR chemical shifts (δ in ppm) and coupling constants (J in Hz) of cyclic peptide **1** in $CDCl_3$ and cyclic peptides **2** and **3** in C_6D_6.

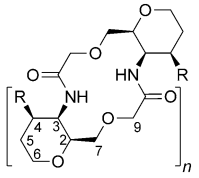

1, *n* = 1, R = OMe
2, *n* = 1, R = H
3, *n* = 3, R = OMe

Protons[a]	**1** ($CDCl_3$)	**2** (C_6D_6)	**3** (C_6D_6)
NH	7.65 (d) (10.4)	7.72 (bd) (7.0)	7.22 (d) (10.1)
C2–H	3.69 (ddd) (10.7, 4.6, 1.0)	2.92 (ddd) (4.6, 4.6, 1.5)	3.20 (ddd) (8.5, 2.4, 1.6)
C3–H	4.53 (dd) (10.4, 3.8)	3.99 (m)	4.50 (dd) (10.0, 4.0)
C4–H_{ax}	3.47 (ddd) (11.7, 4.9, 3.9)	1.19 (dddd) (13.5, 13.5, 3.5, 3.5)	2.89 (ddd) (11.9, 4.5, 4.3)
C4–H_{eq}	–	2.06 (bd) (13.5)	–
C5–H_{ax}	1.74 (dddd) (13.2, 13.2, 11.8, 5.3)	1.54 (ddddd) (13.7, 13.5, 12.8, 4.5, 4.5)	1.67 (dddd) (13.0, 12.9, 12.6, 5.1)
C5–H_{eq}	1.87 (m)	0.82 (bdd) (13.7, 2.0)	1.39 (dd) (13.0, 4.2)
C6–H_{ax}	3.61 (ddd) (12.7, 12.6, 2.6)	2.97 (ddd) (12.7, 11.3, 2.5)	3.03 (ddd) (12.9, 11.7, 2.4)
C6–H_{eq}	4.11 (ddd) (12.1, 5.2, 1.2)	3.56 (dd) (11.2, 5.0)	3.70 (dd) (11.7, 4.1)
OMe	3.34 (s)	–	3.22 (s)
C7–H_{proS}	3.77 (dd) (10.3, 4.6)	3.33 (dd) (10.3, 4.0)	3.51 (dd) (11.0, 2.5)
C7–H_{proR}	3.39 (dd) (10.7, 10.3)	2.99 (dd) (10.3, 5.0)	3.61 (dd) (11.0, 8.5)
C9–H_{proS}	3.87 (d) (16.4)	3.69 (d) (14.7)	3.88 (d) (15.8)
C9–H_{proR}	4.26 (d) (16.4)	3.88 (d) (14.7)	4.05 (d) (15.8)

[a] ax = axial, eq = equatorial.

which could not be used to calculate the rotamer populations around the torsional angle (O1-C2-C7-O8) by applying the Serianni equation system,[23] probably because the most stable conformer is not totally staggered. However, the coupling-constant values imply a great population of one conformer similar to the *gt* staggered conformer (Figure 2). The presence of

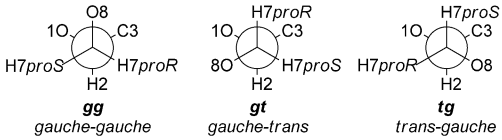

Figure 2. Rotamers around the C7–C2 bond.

a strong NOE interaction between the amide proton and C5–H_{ax} confirms that the amide proton is situated above the sugar ring, which is in agreement with the observed $^3J_{NH-C3H}$ value mentioned above (Figure 3).

Also, strong NOE interactions between the amide proton and C7–H_{proR}, which could be intra- or interresidue, and between C3–H and C7–H_{proS} and between C3–H and C7–H_{proR}, confirm an analogue *gt* staggered rotamer around the C7–C2 bond. Additionally, the stereospecific assignment of C9–H_{proS} and C9–H_{proR} was accomplished from the strong NOE interactions of C9–H_{proS} with C7–H_{proR} and C7–H_{proS} (Figure 3).[24]

FTIR spectroscopic analysis was performed with cyclic dimer **1** in CH_2Cl_2 at different concentrations to obtain more information about the hydrogen-bonding pattern. The IR spectrum of **1** in CH_2Cl_2 displays a sharp amide A absorption (N–H stretching mode) at $\tilde{\nu}=3336\ cm^{-1}$, amide I absorption (mainly C=O stretching mode) at $\tilde{\nu}=1674\ cm^{-1}$, and amide II absorption (mainly N–H bending and C–N stretching mode) at $\tilde{\nu}=1533\ cm^{-1}$, which are independent of the sample concentration in the range 100–5 mM. These results confirm the formation of intramolecular hydrogen bonds.

Cyclodipeptide **1** yielded a single crystal suitable for X-ray analysis,[25] and the crystal structure strongly resembles the solution-phase conformer. The tetrahydropyran rings displayed a chair conformation with substituents in the C2 and C4 equatorial positions and a substituent in the C3 axial position. The dihedral angle between the amide and C3 protons (H-*N*-C3–H) is close to an antiperiplanar arrangement with an average value of $+170^\circ$. Additionally, the torsional angle (O1-C2-C7-O8) with an average value of $+46^\circ$ confirms a not completely staggered conformation similar to the *gt* conformer (Figure 2).[26] However, the most interesting feature of the crystal structure emerged from the close contact established between the amide proton of one residue and the pyran oxygen atom of the other residue, thus forming an eight-membered hydrogen-bonded pseudocycle (C_8), which helps to keep the center ring collapsed and thereby generating a folded structure (Figure 4a). Moreover, this folded structure is also upheld by two

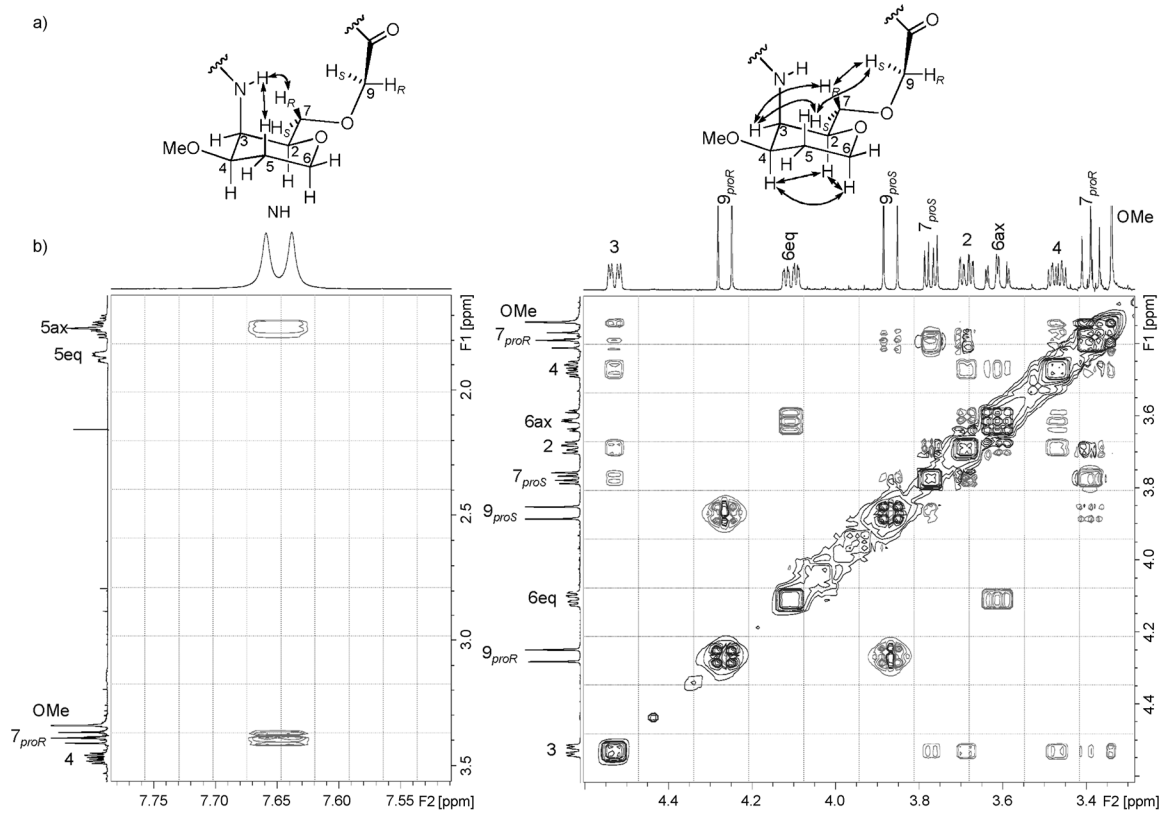

Figure 3. a) Schematic representation of observed NOE interactions of cyclodipeptide **1** in $CDCl_3$. The solid arrows represent strong NOE interactions. Sequential NOE interactions have been omitted for clarity. b) Two-dimensional NOESY sections that show key intraresidue NOE interactions for cyclodipeptide **1** in $CDCl_3$ at 300 K.

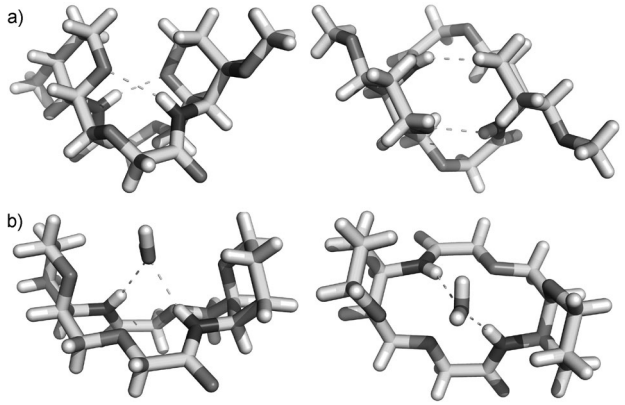

Figure 4. X-ray structure of cyclodipeptides **1** and **2**.[27] a) Side and top views of cyclopeptide **1**. b) Side and top views of cyclopeptide **2**. The dashed lines represent hydrogen bonds.

additional five-membered hydrogen-bonded pseudocycles (C_5) between the amide protons and the ether oxygen atoms of the 2-oxyacetamide groups. This type of hydrogen bonding has been traditionally been considered to be a weak electrostatic interaction. However, there have been some reported examples in which these interactions play a key role in the conformation equilibrium and in the formation of secondary structures.[15] These intramolecular hydrogen bonds explain perfectly the results of the NMR and FTIR spectroscopic experiments.

The conformational change of cyclodipeptide **1** in a more polar environment was checked by dissolving **1** in D_2O and performing ^{1}H NMR, COSY, and NOESY experiments.[24] The ^{1}H NMR spectrum of **1** in D_2O is similar to that observed in $CDCl_3$. However, the most notable change was seen in the coupling-constant values $^3J_{C2H-C7HproR} = 8.1$ and $^3J_{C2H-C7HproS} = 4.5$ Hz. These parameters are quite relevant because they can be considered to be a probe for the degree of the molecular folding. The rotamer populations around the torsional angle (O1-C2-C7-O8) were calculated from the coupling-constant values by applying the Serianni equation system,[23] thus yielding the population of the three staggered conformers of 12, 63, and 25% for *gg*, *gt*, and *tg*, respectively (Figure 2). By comparing these results with those obtained in $CDCl_3$, it is clear that there is an increase in the population of *gg* and *tg* conformers and a decrease in the population of the *gt* conformer in D_2O. Bearing in mind that the *gg* and *tg* conformers are representative of the unfolded structure, it can be assumed that there is a significant conformational change on going from an aqueous to a lipophilic medium.[28] However, the folded conformer *gt* remains the most abundant in the aqueous medium.

Conformational analysis of 2

The cyclic dimer **2** is a 14-membered macrocyclic peptide, which lacks the methoxy groups at C4. However, this small structural change implies large conformational changes. The ^{1}H NMR spectrum of **2** recorded in $CDCl_3$, C_6D_6, and D_2O at 300 K showed a symmetrical set of high-resolution signals. The chemical shifts of the amide proton in C_6D_6 ($\delta_{NH} = 7.72$ ppm) remained constant as the sample concentration was diluted from 25 to 1.0 mM, which suggested that N–H bonds are involved in intramolecular hydrogen bonding. However, the observed $^3J_{NH-C3H}$ value was 7.0 Hz, which corresponds to a torsion angle of H-*N*-C3–H $\approx \pm 142^\circ$. Therefore, the amide protons are pointing to the pyran oxygen atoms of the same residue, thus probably establishing C5–type electrostatic interactions as described above. However, the presence of the methoxy group at C4 in the cyclic peptide **1** competes with the pyran oxygen atom through an interaction of the same type, thereby forcing the amide protons to adopt an antiperiplanar arrangement with respect to the proton at C3 (H-*N*-C3–H $\approx 180^\circ$). Coupling constants and NOE interactions between protons of the pyranose rings confirmed a chair conformation with substituents in the C2 and C4 equatorial positions and a substituent in the C3 axial position. Diastereotopic assignment of the prochiral methylene protons at C7 was carried out on the basis of the $^3J_{2,7}$ coupling constants and NOE interactions. Thus, the coupling-constant values of $^3J_{C2H-C7HproR} = 5.0$ and $^3J_{C2H-C7HproS} = 4.0$ Hz were used to calculate the rotamer populations around the torsional angle (O1-C2-C7-O8) by applying the Serianni equation system.[23] Thus, the calculated populations of the three staggered conformers were 48, 35, and 17% for *gg*, *gt*, and *tg*, respectively (Figure 2). In the two-dimensional NOESY experiment, NOE cross-peaks between the amide proton in C5–H_{ax} and C7–H_{proR} were observed. The former cross-peak confirms that the amide proton is situated above the sugar ring, and the latter peak indicates the contribution of the *gt* conformer around the C2–C7 bond in the conformational population in solution. The stereospecific assignment of C9–H_{proS} and C9–H_{proR} was accomplished from strong NOE interactions between C9–H_{proS} and C7–H_{proR} and between C9–H_{proR} and C7–H_{proS} (Figure 5).

The IR spectrum of cyclopeptide **2** in CH_2Cl_2 displays two sharp amide A absorptions (N–H stretching mode) at $\tilde{\nu} = 3425$ (free) and 3331 cm^{-1} (bond), an amide I absorption at $\tilde{\nu} = 1671$ cm^{-1}, and an amide II absorption at $\tilde{\nu} = 1536$ cm^{-1}, which are independent of the sample concentration in the range 100–5 mM. These results confirm the formation of intramolecular hydrogen bonds. It is noteworthy that there was an absorption band at $\tilde{\nu} = 3186$ cm^{-1}, which is assigned to water involved in the formation of hydrogen bonds.

The X-ray structure of cyclodipeptide **2** strongly resembles one of the conformers found in the solution phase.[25] The tetrahydropyrans rings display the chair conformation with substituents at the C2 and C4 equatorial positions and a substituent at the C3 axial position. The dihedral angle between the amide and C3 protons (H-*N*-C3-H) is approximately equal to -152°.[26] Additionally, the crystal structure exclusively displayed the *gg* conformer around the C2–C7 bond (Figure 4b). However, the most important feature is that cyclodipeptide **2** adopts a U-shaped structure, in which there is a hydrophilic concave face with four oxygen atoms and two amide protons directed toward the center of the cavity. In the center of the cavity, a water molecule is complexed by two hydrogen bonds established between a water oxygen atom and both amide protons (Figure 4b). This U-shaped structure is further stabilized by a trifurcated hydrogen bond between each amide

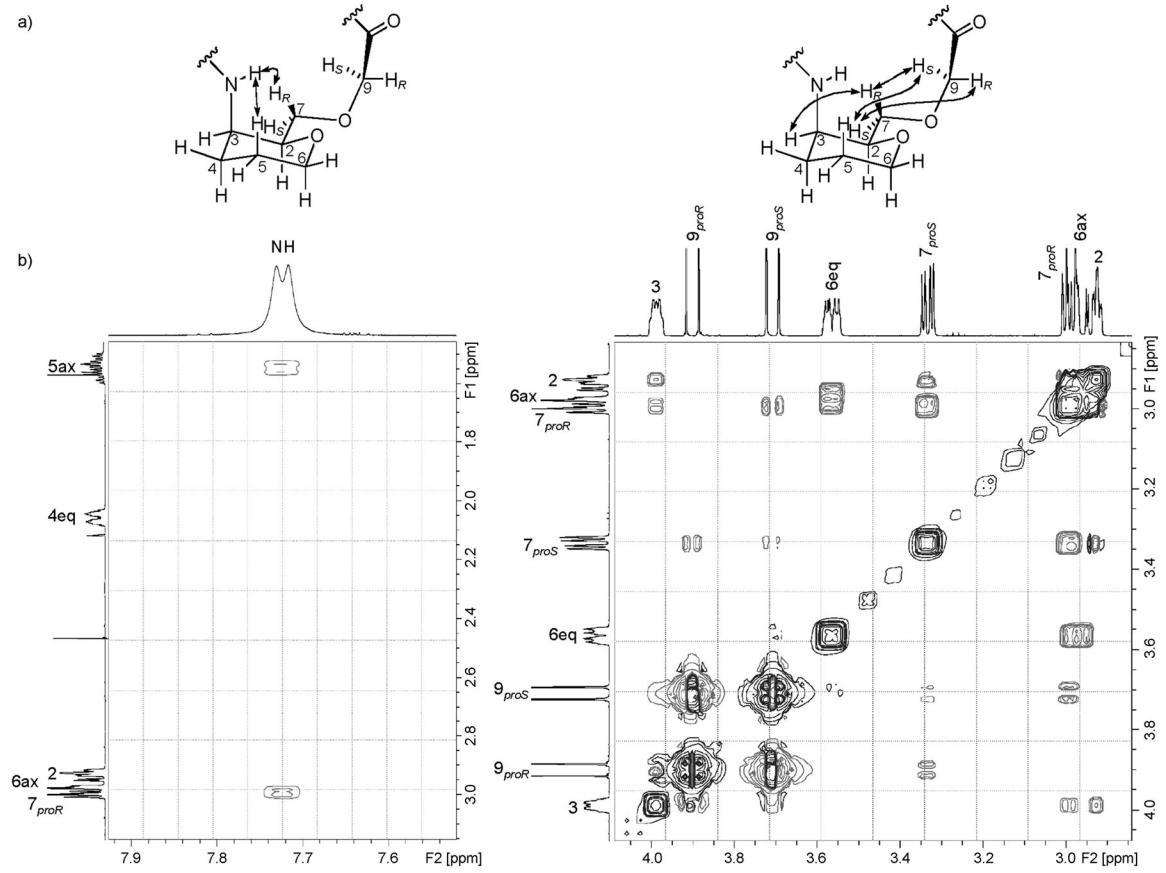

Figure 5. a) Schematic representation of observed NOE interactions of cyclodipeptide **2** in C_6D_6. The solid arrows represent strong NOE interactions. Sequential NOE interactions have been omitted for clarity. b) Two-dimensional NOESY sections that show key intraresidue NOE interactions for cyclodipeptide **2** in C_6D_6 at 300 K.

proton and three hydrogen-bond acceptors: the pyran oxygen atom (C_5) and O8 (C_6) both from the same residue and O8 of the other residue (C_5). This complexation with water explains the results obtained from the NMR and FTIR spectroscopic experiments in the solution phase.

Model acyclic compounds **30**–**32** were synthesized[24] and the FTIR and ^{1}H NMR spectra were studied to confirm the important role of the methoxy group in the conformation equilibrium observed. These compounds represent a structural simplification of cyclic dipeptides **1** and **2**. Additionally, *N*-isopropyl-2-methoxyacetamide was used as a model to study the five-membered-ring hydrogen bond between the amide proton and ether oxygen atom. The IR spectrum of this compound displays one absorption maxima in the N–H stretching region at $\tilde{\nu}=3411\ cm^{-1}$ in CH_2Cl_2 (7 mM) and a chemical shift of the amide proton at $\delta_{NH}=6.31$ ppm in $CDCl_3$ at 7 mM.[29] Compound **30** displays one absorption maxima in the N–H stretching region similar to that observed in *N*-isopropyl-2-methoxyacetamide ($\tilde{\nu}=3417\ cm^{-1}$ in CH_2Cl_2 at 7 mM) and a chemical shift of the amide proton ($\delta_{NH}=6.74$ ppm) in $CDCl_3$ at the same concentration (i.e., 7 mM). Similarly, compound **31** shows one N–H stretching maximum at $\tilde{\nu}=3412\ cm^{-1}$ in CH_2Cl_2 (7 mM), and the N–H signal was slightly shifted downfield with respect to **30** ($\delta_{NH}=6.98$ ppm in $CDCl_3$ at 7 mM). Nonetheless, model compound **32** shows an N–H stretching maximum at $\tilde{\nu}=3438\ cm^{-1}$ and a chemical shift of the amide proton at $\delta=5.62$ ppm, which corresponds to a non-hydrogen-bonded N–H bond. These results clearly indicate that model compounds **30** and **31** have a five-membered hydrogen-bonded pseudocycle (C_5) between the amide protons and ether oxygen of the 2-methoxy acetamide group.[30] Furthermore, the amide proton of **30** displays a large coupling constant with the proton at C3 ($^3J_{NH-C3H}=10.1$ Hz), which corresponds to an antiperiplanar arrangement (H-*N*-C3-H$\approx\pm172^\circ$). This dihedral angle indicates an arrangement of the amide proton almost identical to that observed in the X-ray structure of cyclodipeptide **1** (Figure 6). Conversely, amide **31** displays a coupling constant of the proton at C3 of $^3J_{NH-C3H}=8.3$ Hz, which corresponds to a dihedral angle of H-*N*-C3-H$\approx\pm151^\circ$. According to these values and by taking into account the lack of the methoxy group at C4, the amide proton is placed closer to the pyran oxygen atom, thus favoring an additional C_5 interaction[15e,g] (Figure 6). Therefore, the results obtained from the acyclic models are in perfect agreement with those obtained from the cyclic peptides. These models also allow us to explain the role of the methoxy group in the conformation of the cyclopeptides: When there is no methoxy group, the amide protons form a bifurcated hydrogen bond (two C_5), thus forcing the structure to remain unfolded, as in cyclodipeptide **2**; on the contrary, the

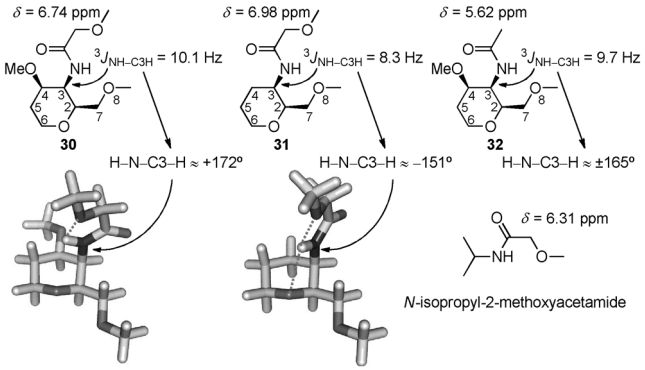

Figure 6. Structures, coupling constants ($^3J_{NH-C3H}$), dihedral angles (H-N-C3-H), and chemical shifts of the amide proton in $CDCl_3$ (7 mM) of the model compounds **30**–**32** and *N*-isopropyl-2-methoxyacetamide.

methoxy group at C4 induces a change in the dihedral angle (H-*N*-C3-H), thereby favoring the folding of cyclodipeptide **1**.

On the other hand, the existence or otherwise of additional interactions between the NH bond and pyran oxygen atom could also help to explain why the macrocyclization reaction failed to provide cyclic tetrapeptide **4**, whereas this reaction worked well to give macrotetrapeptide **3**. The cyclization precursor **25** displayed coupling values of $^3J_{NH-C3H} = 8.7$, 9.1, and 9.3 Hz (dihedral angles: H-*N*-C3-H ≈ -154–-160°), a chemical shift of $\delta_{NH} = > 7.15$ ppm in $CDCl_3$, and a major band at $\tilde{\nu} = 3415\ cm^{-1}$ in the FTIR spectrum in CH_2Cl_2 at 7 mM. These values clearly indicate the formation of a bifurcated hydrogen bond ($2\times C_5$) of the NH bond in each residue, in which two hydrogen-bond acceptors participate, namely, the pyran oxygen atom of residue *i* and O8 of residue *i*−1. These interactions could stabilize a twist–turn conformation, which puts the extremes of the molecule far away, therefore increasing the propensity for oligomerization instead of cyclization. Conversely, the cyclization precursor **19** displayed coupling values of $^3J_{NH-C3H} = 9.8$, 10.2, and 10.3 Hz (dihedral angles: H-*N*-C3-H $\approx +167$–179°), a chemical shift of $\delta_{NH} = < 6.86$ ppm in $CDCl_3$, and a major band at $\tilde{\nu} = 3422\ cm^{-1}$ in CH_2Cl_2 at 7 mM. Thus, the absence of bifurcated hydrogen bonds produces a more flexible molecule, in which both ends could be found, thus leading to the cyclized product **3**.

Conformational changes induced in cyclodipeptide **2** by changing from $CDCl_3$ to D_2O were determined by comparison of the coupling-constant values $^3J_{C2H-C7HproR}$ and $^3J_{C2H-C7HproS}$ obtained from the ^1H NMR spectra, which yielded three staggered conformers around the torsional angle (O1-C2-C7-O8) by using the Serianni equation system.[23] The populations obtained in $CDCl_3$ ($^3J_{C2H-C7HproR} = 6.4$ and $^3J_{C2H-C7HproS} = 4.1$ Hz) were 33, 48 and 19% for the *gg*, *gt*, and *tg* conformers, whereas the equations provided 70, 16, and 14% for the *gg*, *gt*, and *tg* conformers in D_2O ($^3J_{C2H-C7HproR} = 3.0$ and $^3J_{C2H-C7HproS} = 3.9$ Hz).[24] The conformation of cyclodipeptide **2** was more sensitive to the change of the medium than it's the analogous cyclodipeptide **1**; that is, the folded and unfolded conformers of cyclodipeptide **2** are in equal proportion in $CDCl_3$, whereas 84% (*gg* + *tg*) of the conformers are unfolded and only 16% (*gt*) are folded in D_2O.

Conformational analysis of 3

The cyclic tetramer **3** is a 28-membered macrocyclic peptide. In this case, the ^1H NMR spectrum in C_6D_6 also showed a symmetrical set of high-resolution signals, which could be due to a rigid conformation with C_4 symmetry, two interconvertible structures with C_2 symmetry, or a structure involved in a fast conformation equilibrium on the NMR timescale. Coupling constants indicated a chair conformation of the pyranose rings with substituents at the C2 and C4 equatorial positions and a substituent at the C3 axial position. The chemical shift of the amide proton ($\delta_{NH} = 7.22$ ppm in C_6D_6) suggested that the N–H bond could be involved in weak hydrogen bonds. Also, this chemical shift remained constant as the sample concentration was diluted in $CDCl_3$ from 22.8 to 0.68 mM ($\delta_{NH} = 7.12$ ppm), thus suggesting there is no aggregation in $CDCl_3$ and ruling out the presence of intermolecular hydrogen bonds. Additionally, the values of the temperature coefficient of the N–H bond in $CDCl_3$ in a range from 249 to 300 K ($\Delta\delta/\Delta T = -3.0$ ppb K^{-1}) confirms the formation of intramolecular hydrogen bonds.[31] The amide proton exhibits a large coupling constant with the proton at C3 ($^3J_{NH-C3H} = 10.1$ Hz), which corresponds to an antiperiplanar arrangement (H-*N*-C3-H $\approx \pm 172^\circ$). The coupling-constant values of $^3J_{C2H-C7HproR} = 8.5$ and $^3J_{C2H-C7HproS} = 2.5$ Hz were used to calculate the rotamer populations around the torsional angle (O1-C2-C7-O8) by applying the Serianni equation system.[23] Thus, the calculated populations of the three staggered conformers were 22, 76, and 2% for *gg*, *gt*, and *tg* (Figure 2). Due to the symmetry of the spectrum, it is not possible a priori to discriminate between the intra- and interresidue NOE interactions. In addition to the typical NOE interactions from the pyranose chair conformation, there were other strong NOE interactions between the amide proton and C5–H_{ax} and C7–H_{proR} and between C3–H and C7–H_{proS} (Figure 7). The former result indicated that the amide proton is positioned above the sugar ring, which is in agreement with the observed $^3J_{NH-C3H}$ value mentioned above. The latter data confirmed the high percentage of the *gt* conformer. Also, weak NOE interactions between C3–H and C7–H_{proR} corroborated the presence of the *gg* conformer. Probably, the most flexible part of the cyclic tetramer **4** is at position C9. Nonetheless, medium NOE interactions were observed between C2–H and C9–H_{proR}, between C7–H_{proS} and C9–H_{proR}/C9–H_{proS}, and between C7–H_{proR} and C9–H_{proS}, which indicates that the C9–H_{proS} bond is on the bisector of the angle between the protons located at C7 and also that C9–H_{proR} is antiperiplanar to C7–H_{proR} (Figure 7). Unfortunately, all attempts to crystallize macrotetrapeptide **3** were unfruitful.

FTIR spectroscopy was performed with cyclic tetramer **3** in dilute CH_2Cl_2 (7 mM). Under these conditions, hydrogen bonding is directly detectable from the N–H stretching region. The IR spectrum of **3** displays three absorption maxima in the N–H stretching region at $\tilde{\nu} = 3414$, 3388, and 3350 cm^{-1}. The new model acyclic compounds **33** and **34** were synthesized,[24] and the ^1H NMR and FTIR spectra of the reference compounds **30** and **32**–**34** were examined at the same concentration (Figure 8) to determine the type of hydrogen bond formed.

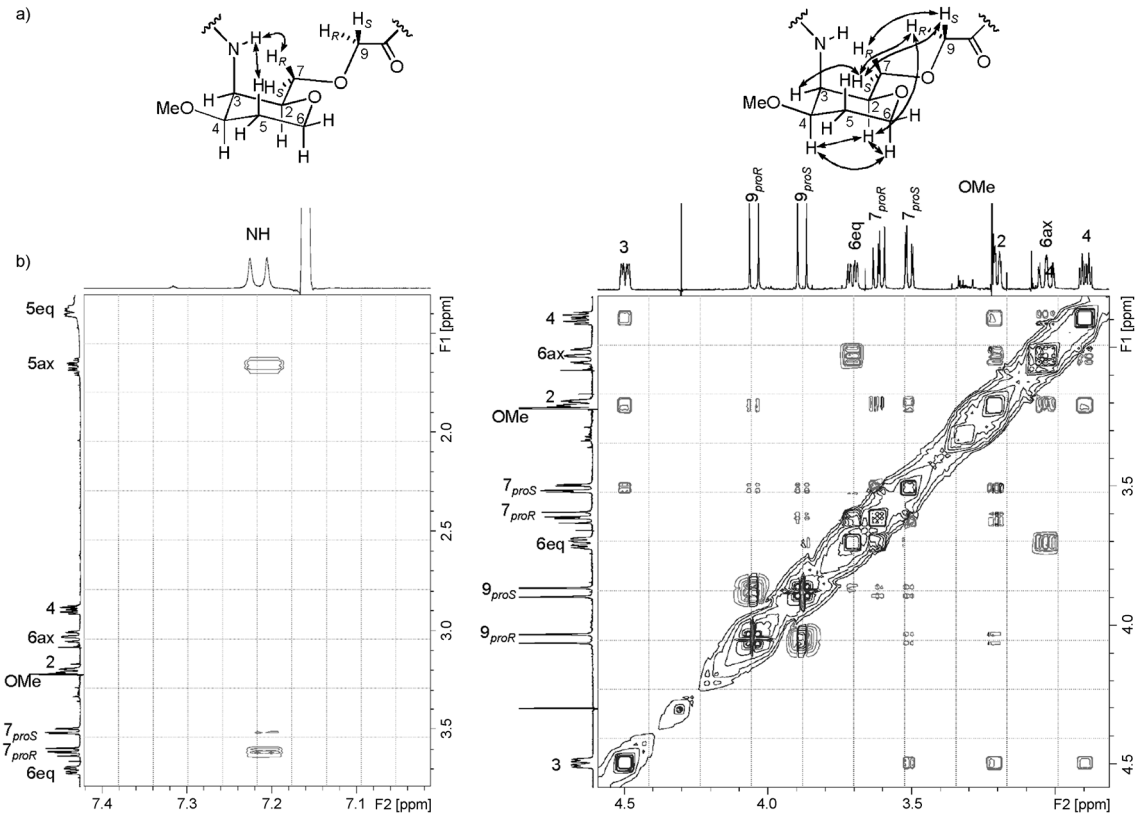

Figure 7. a) Schematic representation of observed NOE interactions of macrotetrapeptide **3** in C_6D_6. The solid arrows represent strong NOE interactions. Sequential NOE interactions have been omitted for clarity. b) Two-dimensional NOESY sections showing key intraresidue NOE interactions for macrotetrapeptide **3** in C_6D_6 at 300 K.

These compounds represent a structural simplification of cyclic tetrapeptide **3**. As it was mentioned before, acetamide **32** shows only one N–H stretching maximum at $\tilde{\nu}=3438\ cm^{-1}$ and a chemical shift of the amide proton of $\delta_{NH}=5.62$ ppm, which corresponds to a non-hydrogen-bonded NH group. Also, amide **30** displays one N–H stretching maximum at $\tilde{\nu}=3417\ cm^{-1}$ and a chemical shift of the amide proton at $\delta_{NH}=6.74$ ppm, which may be attributed to a five-membered hydrogen-bonded pseudocycle (C_5) between the amide proton and the ether oxygen atom of the 2-metoxyacetamide. Compound **33** only has the chance to form a conventional nine-membered-ring hydrogen bond between the amide proton of the acetamide group and the carbonyl group of the piperidine amide. However, in the N–H stretching region only one maximum appears at $\tilde{\nu}=3437\ cm^{-1}$ and a chemical shift of the amide proton of $\delta_{NH}=5.76$ ppm, which corresponds to a non-hydrogen bonded NH group. Furthermore, the model compound **34** has two amide protons that can form conventional 9- and 11-membered hydrogen-bonded pseudocycles (C_9 or C_{11}) and weak electrostatic interactions (C_5). The FTIR spectrum in the N–H stretching region shows three maxima: one major band at $\tilde{\nu}=3415\ cm^{-1}$, which corresponds to the weak electrostatic interactions, and two bands at $\tilde{\nu}=3351$ and $3325\ cm^{-1}$, which arise from the 9- and 11-membered hydrogen-bonded pseudocycles (Figure 8). Therefore, these results confirm the existence of weak electrostatic interactions, such as C_5, between the NH bond and the ether oxygen atoms in cyclic tetrapeptide **3**, and they also indicate the presence of intramolecular conventional hydrogen bonds.

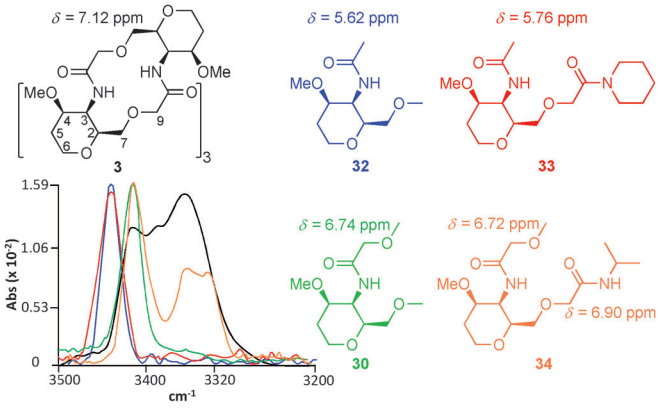

Figure 8. Structures, partial IR spectra in CH_2Cl_2 (7 mM), and chemical shifts in $CDCl_3$ (7 mM) of macrotetrapeptide **3** and the reference compounds **30** and **32**–**34**.

Molecular modeling

A theoretical conformation analysis was performed to gain insight into the conformation equilibrium observed in these cyclic peptides. A conformation search was done by using a mixed torsional/low-mode conformational search,[32] which has proved to be very useful in conformation searches of

medium-size rings. It was used as implemented in the Maestro version 9.3[33]/Macromodel version 9.9[34] by using either $CHCl_3$ or water as specified in the text. The best force field (FF) to suit our molecules was OPLS 2001[35] among all those implemented on MacroModel with only two medium quality torsion parameters (Osp^2-Csp^2-Csp^3-Osp^3) against all the other 156/114/60 high-quality torsion/bending/stretching parameters. Charges were provided from the FF with an extended cutoff. Conformers were minimized by using the truncated Newton conjugate gradient (TNCG) method with a gradient convergence within a threshold of 0.005. A maximum numbers of steps of 10000 was the limit within an energetic range of 21.0 kJ mol^{-1} (5.02 kcal mol^{-1}) to ensure that all the conformational space was mapped. Significant conformation differences between cyclodipeptides **1** and **2** were observed when the solvent was changed from $CHCl_3$ to water, but these compounds are better discussed if a definition of folded geometry in such systems is proposed. First, a reference system was taken. It is reasonable to consider the crystal structure of cyclic peptide **1** as the folded reference (Figure 4a). Second, a good parameter to follow the folding of the cyclic peptides is required. The crystal structure of cyclic peptide **1** displays a folded structure, and the collapsed structure is mainly due to the formation of two eight-membered hydrogen-bonded pseudocycles (C_8) between the amide proton of one residue and the pyran oxygen atom of the other residue. Consequently, the distance between the amide proton of one residue and the pyran oxygen atom of the other residue defines quite well the folding degree, and therefore it was considered to be the geometrical parameter of folding, which is on average 2.28 Å measured on the reference system. This value was considered to be the geometrical reference of folding. Finally, a borderline was set at 2.7 Å, which includes a top margin of almost 20% with respect to the folding reference value, to define what a folded conformer is. Thus, the cyclodipeptide is considered to be folded if the distance between those selected positions is smaller than 2.7 Å, and it is considered to be unfolded if the distance is larger. According to this parameter, a prevalence of folded conformers in the cyclic peptide **1** either in $CHCl_3$ or water with respect to the cyclic peptide **2** is clearly seen. Indeed, among the conformers found within a range of 21 kJ mol^{-1} from the global minimum (Figure 9) in $CHCl_3$, 30 out of 39 conformers of cyclic peptide **1** (77%) are folded, whereas they represent only 10 out of 22 conformers of cyclic peptide **2** (45%). However, among the conformers found within a range 21 kJ mol^{-1} from the global minimum in water (Figure 9), 32 out of 88 conformers of cyclic peptide **1** (36%) are folded, whereas they represent only 8 out of 40 conformers of cyclic peptide **2** (20%). Moreover, cyclic peptide **1** displays the first unfolded structure in $CHCl_3$ at 9.80 kJ mol^{-1} with respect to its global minimum, whereas cyclic peptide **2** displays this structure at 1.48 kJ mol^{-1}. Nonetheless, although the folded structures still are the most stable in water, the energy gap between the first folded and the first unfolded conformers decreases noticeably. Thus, this value is 3.91 kJ mol^{-1} for cyclic peptide **1** and is just 0.88 kJ mol^{-1} for cyclic peptide **2**. These theoretical calculations clearly confirm the results obtained from the NMR spectroscopic experiments, in which it was established that the proportions between the populations of the *gg*, *gt*, and *tg* conformers can be used as a parameter to determine the degree of folding.

In the case of macrotetrapeptide **3**, the conformation search displays a collapsed structure as the most stable conformer (Figure 9d). Also, the conformers found within a range of 10 kJ mol^{-1} from the global minimum show similar three-dimensional structures (Figure 9), all of them with the pyranose rings in a chair conformation, in which the substituents at C2 and C4 are in the equatorial position and the substituent at C3 is in the axial position. The structure is collapsed mainly by the formation of an 11-membered hydrogen-bonded pseudocycle (C_{11}) between the amide proton of residue *i* and the carbonyl group of residue *i*−2, which is present in all the conformers in the range of 10 kJ mol^{-1}. This hydrogen bond explains the absorption maximum in the N–H stretching region at $\tilde{\nu}=$ 3350 cm^{-1} (Figure 8). The second most stable conformer displays an eight-membered hydrogen bonded pseudocycle (C_8) between the amide proton of residue *i* and the pyran oxygen atom of residue *i*−1, which explains the absorption maximum in the N–H stretching region at $\tilde{\nu}=3388$ cm^{-1} (see Figure S1 in the Supporting Information). Additionally, other types of intramolecular hydrogen bonds, such as interresidue five-membered hydrogen-bonded pseudocycle (C_5) interactions between the oxygen atom of the linker and the N–H bond of the amide groups, are present. These theoretical results confirm those obtained by IR spectroscopic analysis and can also explain how the ^{1}H NMR spectrum shows a symmetrical set of high-resolution signals, which corresponds to a structure involved in a fast conformation equilibrium on the NMR timescale.

Conclusion

In summary, new pyranoid ε-sugar amino acids (ε-SAAs) were designed as building blocks for the synthesis of cyclic peptide homooligomers. Those ε-SAAs have proven to be privileged scaffolds for the synthesis of conformationally modulated cyclic peptides. Indeed, the sugar unit allows control of the disposition and configuration of several moieties that are susceptible to acting as conformational modulators. Remarkably, the carboxylic acid and the amine groups are placed at C2 and C3 with respect to the pyran oxygen atom in these ε-SAAs. This disposition allows such an oxygen atom to participate actively in the control of the intramolecular hydrogen-bonding pattern, and therefore to affect the conformation equilibria. Also, the carboxylic acid and sugar moieties are linked through an ether group. The ether oxygen atom and pyran oxygen atom participate in five-membered hydrogen-bonded pseudocycle (C_5) interactions, and the N–H bonds of the amide groups help to create an internal backbone of hydrogen bonds in the cyclic peptides. The influence of an additional control element on the sugar moiety in the conformation equilibrium was also studied, namely, a methoxy group at C4, which plays an important role in the populations of the folded and unfolded conformers. Thus, when the methoxy group is

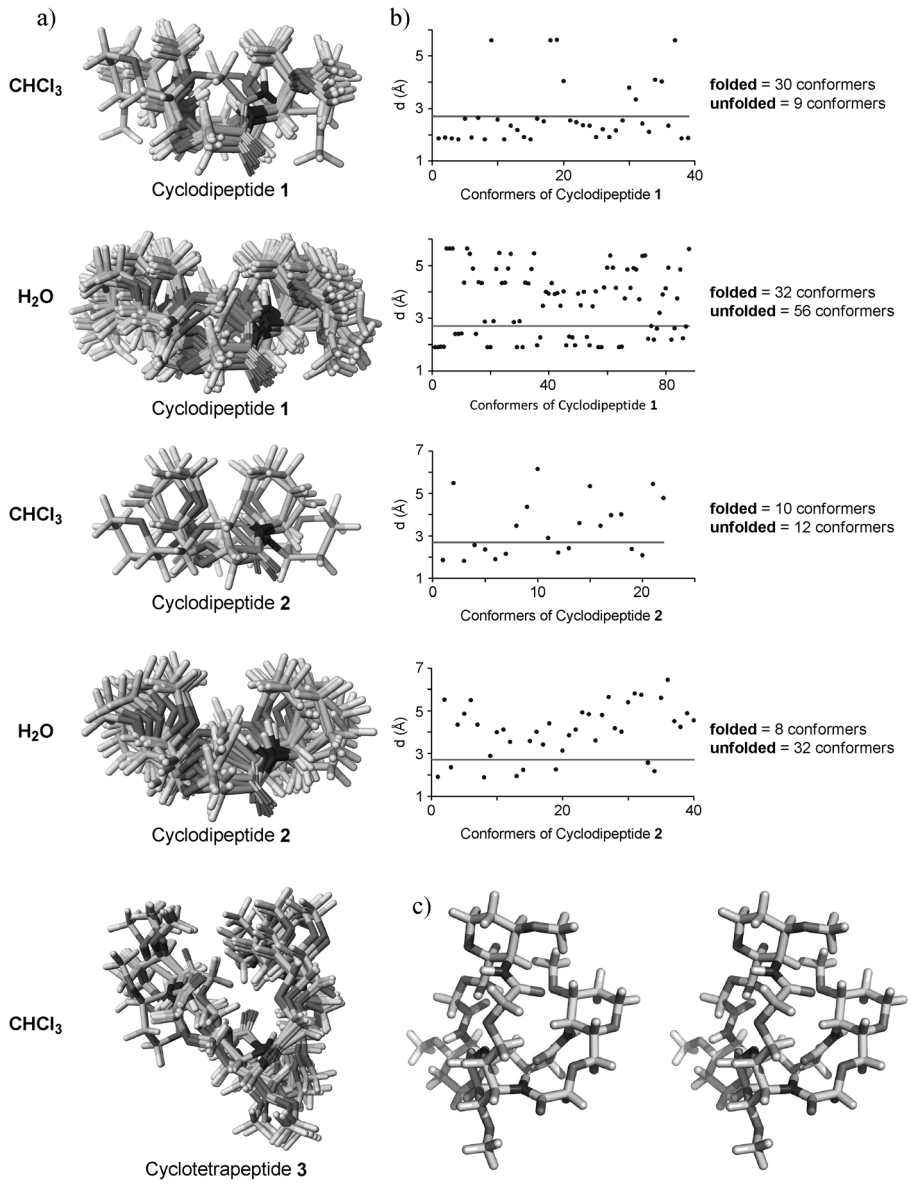

Figure 9. a) Clustering of conformers within 10 kJ mol^{-1} from the global minimum (for ease of visualization only). b) Representation of all the conformers found within 21 kJ mol^{-1} from the global minimum versus the geometrical parameter of folding *d* (the interresidue distance [Å] between the pyran oxygen atom and amide proton). The borderline was set at 2.7 Å, thus all the conformers below that value are considered to be folded and vice versa. c) A stereoview of the minimum-energy structure of cyclotetrapeptide **3**. The dashed line represents a hydrogen bond (C_{11}).

present in cyclodipeptides, the folded conformation is the most abundant in nonpolar and polar environments, with only small differences in the conformation population between both media. However, when there is no methoxy group, the folded and unfolded conformers are in equal proportion in a nonpolar environment, but the unfolded conformers are present almost exclusively in an aqueous medium. These results are mainly due to a change in the dihedral angle between the amide proton and the proton at C3 (H-*N*-C3-H) induced by the methoxy group. In all the cases, the oxygen atom of the linker forms an interresidue five-membered hydrogen-bonded pseudocycle (C_5) interaction with the N–H bond of the amide group. When the methoxy group is absent, the formation of an additional intraresidue five-membered hydrogen-bonded pseudocycle (C_5) with the pyran oxygen atom is favored, thus generating a system of bifurcated hydrogen bonding ($2\times C_5$), and this internal network of noncovalent interactions helps to stabilize the unfolded structures. However, when the methoxy group is present, the torsion angle (H-*N*-C3-H) changes and the pyran oxygen atom is instead involved in an interresidue eight-membered hydrogen-bonded pseudocycle (C_8), and therefore a folded structure is formed. This methoxy group not only influences the conformation equilibrium, it also affects the reactivity of the molecules. Indeed, the macrocyclization reaction takes place in the synthesis of the cyclotetrapeptides when such appendix on the sugar moiety is present; however, the absence of this unit prevents the reaction. These results highlight how subtle structural changes can completely alter the pattern of noncovalent interactions and induce conformational changes that affect the properties of cyclopeptides. Therefore, the introduction of this type of appendix as a conformation-control element can be considered to be a useful tool in the design of novel cyclic peptides because the formation of folded conformations, which usually have higher passive permeability, is promoted, therefore improving bioavailability.

Experimental Section

Materials and general methods

The ^{1}H NMR spectra were recorded at 500 or 400 MHz; ^{13}C NMR spectra were recorded at 100 or 125 MHz; and the chemical shifts are reported in ppm and referenced to the solvent peak. Melting points were taken on a capillary melting-point apparatus and are uncorrected. Optical rotations were obtained on a polarimeter at $\lambda = 589$ nm at 25 °C with a path length of 10 cm and a volume of 1.0 mL. Concentration (*c*) is reported in grams per 100 mL of the solvent specified. Infrared (FTIR) spectra are reported in wavenum-

bers (cm^{-1}). Low- and high-resolution mass spectra were recorded on TOF analyzer mass spectrometers by using electrospray ionization (ESI+) or electron impact (EI) at 70 eV, as specified in each case. Column chromatography was performed on silica gel (60 Å and 0.2–0.5 mm). Compounds were visualized by use of UV light, 2.5% phosphomolybdic acid in ethanol, or vanillin with acetic and sulfuric acid in ethanol with heating. All the solvents were purified by using standard techniques.[36] Reactions requiring anhydrous conditions were performed under nitrogen. Anhydrous magnesium sulfate was used for drying solutions.

tert-Butyl 2-{[(2*R*,3*S*,4*R*)-3-(benzyloxy)-4-methoxytetrahydro-2*H*-pyran-2-yl]methoxy}acetate (10)

A 1 M solution of borane tetrahydrofuran complex in THF (87.9 mL, 87.9 mmol) was added to benzylidene acetal **9**[18] (4.4 g, 17.58 mmol) dissolved in CH_2Cl_2 (176 mL) at room temperature under nitrogen. The reaction mixture was stirred for 10 min, and freshly dried copper(II) trifluoromethanesulfonate (318 mg, 0.88 mmol) was added portionwise to the solution. After stirring for a period of time (2 h), the mixture was cooled to 0 °C, and the reaction was quenched by sequential additions of triethylamine (2.45 mL, 17.58 mmol) and methanol (caution: hydrogen gas was evolved). The resulting mixture was concentrated at reduced pressure followed by coevaporation with methanol. The residue was purified by flash column chromatography on silica gel to give the expected primary alcohol (4.35 g, 98% yield). ^{1}H NMR (400 MHz; $CDCl_3$): δ = 1.46 (ddd, J = 12.9, 11.0, 5.1 Hz; 1H), 2.00 (ddd, J = 13.1, 4.2, 9.0 Hz; 1H), 3.14 (ddd, J = 8.9, 5.0, 2.7 Hz; 1H), 3.24 (dd, J = 17.7, 8.7 Hz; 1H), 3.3 (m; 2H), 3.37 (s; 3H), 3.58 (dd, J = 11.7, 5.1 Hz; 1H), 3.74 (dd, J = 11.7, 2.9 Hz; 1H), 3.88 (ddd, J = 11.7, 5.0, 1.7 Hz; 1H), 4.55 (d, J = 11.1 Hz; 1H), 4.81 (d, J = 11.1 Hz; 1H), 7.23 ppm (m; 5H); ^{13}C NMR (100 MHz; $CDCl_3$): δ = 30.9 (t), 56.9 (q), 62.7 (t), 65.5 (t), 74.9 (t), 79.8 (d), 82.9 (d), 127.7 (d), 128.0 (d), 128.4 (d), 138.6 ppm (s).

NaH (60% in mineral oil, 0.76 g, 19.02 mmol) was added to a solution of the primary alcohol (4.00 g, 15.85 mmol) in THF (20 mL) at 0 °C stirring for 5 min and was added portionwise to a solution of *tert*-butylbromoacetate (3.51 mL, 23.78 mmol) in THF (60 mL) at 0 °C. The reaction mixture was allowed to warm to room temperature and stirred for 2 h (monitored by TLC analysis). The reaction mixture was cooled to 0 °C and quenched by a slow addition of water. The reaction mixture was extracted with EtOAc (3×50 mL), the organic layer was dried over $MgSO_4$, the solvent was removed under reduced pressure, and the crude product was purified by column chromatography to give **10** (5.17 g, 89% yield) as an oil. $[\alpha]_D^{25}$ = +3.1 (c = 1.1, $CHCl_3$); ^{1}H NMR (400 MHz; $CDCl_3$): δ = 1.46 (s; 9H), 1.59 (m; 1H), 2.07 (m; 1H), 3.37 (m; 4H), 3.45 (s; 3H), 3.73 (dd, J = 10.4, 4.5 Hz; 1H), 3.80 (dd, J = 10.4, 1.6 Hz; 1H), 3.99 (s; 2H), 4.00 (m; 1H), 4.68 (d, J = 11.1 Hz; 1H), 4.90 (d, J = 11.1 Hz; 1H), 7.27 (m; 1H), 7.34 ppm (m; 4H); ^{13}C NMR (100 MHz; $CDCl_3$): δ = 28.1 (q), 30.7 (t), 56.8 (q), 65.6 (t), 69.3 (t), 71.0 (t), 74.8 (t), 78.2 (d), 79.3 (d), 81.4 (s), 83.1 (d), 127.5 (d), 128.0 (d), 128.3 (d), 138.8 (s), 169.5 ppm (s); IR (film, NaCl plates): $\tilde{\nu}$ = 3061, 1746, 1722, 1605, 1088 cm^{-1}; HRMS (ESI): *m/z*: calcd for $C_{20}H_{30}O_6Na$ $[M+Na]^+$: 389.1940; found: 389.1940.

tert-Butyl 2-{[(2*S*,3*R*,4*R*)-3-azido-4-methoxytetrahydro-2*H*-pyran-2-yl]methoxy}acetate (5)

Compound **10** (5 g, 13.7 mmol) was added into a suspension of 5 wt% Pd/C (catalytic) in methanol (90 mL), stirring for 1–3 h (monitored by TLC analysis) at room temperature under 1 atm of H_2 pressure. The reaction mixture was filtered through Celite, washed with methanol (2×25 mL), and the filtrate was collected. Removal of the solvents by rotary evaporation afforded the expected secondary alcohol, which was used without purification. DIAD (4.1 mL, 20.6 mmol), DPPA (4.4 mL, 20.6 mmol), and triphenyl phosphine (5.4 g, 20.6 mmol) were added successively to a solution of secondary alcohol in THF (70 mL) at 0 °C. The reaction mixture was stirred for 10 min and then warmed to reflux for 1 h. The reaction mixture was cooled to room temperature and quenched by the addition of water. The reaction mixture was extracted with EtOAc (3×50 mL), the organic layer was dried over $MgSO_4$, the solvent was removed under reduced pressure, and the crude product was purified by column chromatography to give **5** (3.92 g, 95% yield) as an oil. $[\alpha]_D^{25}$ = +2.9 (c = 1.4 in $CHCl_3$); ^{1}H NMR (400 MHz; $CDCl_3$): δ = 1.46 (s; 9H), 1.77 (m; 1H), 1.95 (dddd, J = 12.6, 12.6, 12.6, 5.1 Hz; 1H), 3.38 (m; 1H), 3.43 (s; 3H), 3.48 (ddd, J = 11.6, 4.6, 3.4 Hz; 1H), 3.54 (ddd, J = 6.2, 6.2, 1.2 Hz; 1H), 3.64 (ddd, J = 14.0, 9.4, 6.1 Hz; 2H), 3.97 (d, J = 16.5 Hz; 1H), 4.00 (m; 1H), 4.02 (d, J = 16.5 Hz; 1H), 4.03 ppm (m; 1H); ^{13}C NMR (100 MHz; $CDCl_3$): δ = 27.0 (t), 28.1 (q), 55.8 (q), 58.7 (d), 66.1 (t), 69.1 (t), 71.2 (t), 76.3 (d), 79.2 (d), 81.7 (s), 169.4 ppm (s); IR (CH_2Cl_2): $\tilde{\nu}$ = 2983, 2106, 1746, 1265, 1103 cm^{-1}; HRMS (ESI): *m/z*: calcd for $C_{13}H_{23}N_3O_5Na$ $[M+Na]^+$: 324.1535; found: 324.1529.

tert-Butyl 2-{[(2*R*,3*S*)-3-hydroxytetrahydro-2*H*-pyran-2-yl]methoxy}acetate (11)

A solution of the diol **8** (1.00 g, 7.57 mmol) in THF (5 mL) was added to a suspension of NaH (60% in mineral oil, 303 mg, 7.57 mmol) in dry THF (10 mL) at 0 °C, and the reaction mixture was stirred for 5 min. A solution of *tert*-butylbromoacetate (1.12 mL, 7.57 mmol) in THF (20 mL) at 0 °C was added portionwise, and the reaction mixture was stirred for a further 2 h (monitored by TLC analysis). The reaction mixture was quenched by the slow addition of water. The reaction mixture was extracted with EtOAc (3×20 mL), the organic layer was dried over $MgSO_4$, the solvent was removed under reduced pressure, and the crude product was purified by column chromatography to give **11** (1.12 g, 60% yield) as an oil. $[\alpha]_D^{25}$ = +47.8 (c = 1.2 in $CHCl_3$); ^{1}H NMR (400 MHz; $CDCl_3$): δ = 1.46 (s; 9H), 1.46 (m; 1H), 1.61–1.78 (m; 2H), 2.13 (m; 1H), 3.15 (ddd, J = 9.0, 3.3, 3.3 Hz; 1H), 3.35 (ddd, J = 11.6, 11.6, 3.0 Hz; 1H), 3.67 (dd, J = 9.8, 3.2 Hz; 1H), 3.80 (dd, J = 9.9, 3.4 Hz; 1H), 3.80 (m; 1H), 3.88 (d, J = 17.1 Hz; 1H), 3.92 (m; 1H), 3.99 (d, J = 3.5 Hz; 1H), 4.09 ppm (d, J = 17.1 Hz; 1H); ^{13}C NMR (100 MHz; $CDCl_3$): δ = 26.0 (t), 28.5 (q), 31.8 (t), 67.5 (d), 68.4 (t), 68.6 (t), 71.9 (t), 81.7 (d), 82.9 (s), 171.2 ppm (s); IR (film, NaCl plates): $\tilde{\nu}$ = 3483, 2978, 2944, 2859, 1731, 1371, 1266, 1152 cm^{-1}; HRMS (ESI): *m/z*: calcd for $C_{12}H_{22}O_5Na$ $[M+Na]^+$: 269.1365; found: 269.1368.

{(2*R*,3*S*)-3-[(Methylsulfonyl)oxy]tetrahydro-2*H*-pyran-2-yl}-methyl benzoate (12)

Triethylamine (10.5 mL, 75.7 mmol) was added to **8** (5 g, 37.8 mmol) dissolved in CH_2Cl_2 (190 mL, 0.2 M) at 0 °C. Benzoyl chloride (4.4 mL, 37.8 mmol) was added to the mixture. After stirring for 30 min, triethylamine (10.5 mL, 75.7 mmol) and methanesulfonyl chloride (2.93 mL, 37.8 mmol) were sequentially added and the mixture was stirred overnight at room temperature. The reaction mixture was quenched by the addition of water (100 mL). The reaction mixture was extracted with CH_2Cl_2 (3×50 mL), the organic layer was dried over $MgSO_4$, the solvent was removed under reduced pressure, and the crude product was purified by column chromatography to give **12** (10.8 g, 92% yield) as an oil. $[\alpha]_D^{25}$ = +7.9 (c = 1.7 in $CHCl_3$); ^{1}H NMR (400 MHz; $CDCl_3$): δ = 1.79 (m; 3H),

2.47 (m; 1H), 3.01 (s; 3H), 3.42 (m; 1H), 3.60 (ddd, J=9.5, 4.6, 2.2 Hz; 1H), 3.98 (m; 1H), 4.44 (dd, J=12.2, 4.6 Hz; 1H), 4.61 (dd, J=12.2, 2.1 Hz; 1H), 4.69 (ddd, J=9.8, 9.8, 4.8 Hz; 1H), 7.44 (dd, J=7.5, 7.5 Hz; 2H), 7.56 (ddd, J=7.3, 7.3, 1.3 Hz; 1H), 8.06 ppm (m; 2H); ^{13}C NMR (100 MHz; $CDCl_3$): δ=25.5 (t), 31.3 (t), 39.2 (q), 63.9 (t), 68.2 (t), 75.4 (d), 77.7 (d), 128.9 (d), 130.2 (d), 130.3 (s), 133.5 (d), 166.7 ppm (s); IR (film, NaCl plates): $\tilde{\nu}$=3063, 2951, 2862, 1723, 1176, 957 cm^{-1}; HRMS (ESI): *m/z*: calcd for $C_{14}H_{18}O_6SNa$ $[M+Na]^+$: 337.0722; found: 337.0729.

[(2*S*,3*R*)-3-Azidotetrahydro-2*H*-pyran-2-yl]methyl benzoate (13)

Sodium azide (10.3 g, 159.1 mmol) was added to **12** (10 g, 31.8 mmol) dissolved in DMF (80 mL, 0.4 M) at room temperature. The reaction mixture was stirred for 10 min and then warmed to 110 °C overnight. The reaction mixture was cooled to room temperature and quenched by the addition of water. The reaction mixture was extracted with CH_2Cl_2 (3×50 mL), the organic layer was dried over $MgSO_4$, the solvent was removed under reduced pressure, and the crude product was purified by column chromatography to give **13** (7.1 g, 85% yield) as an oil. $[\alpha]_D^{25}=-16.9$ (c=1.4 in $CHCl_3$); ^{1}H NMR (400 MHz; $CDCl_3$): δ=1.49 (m; 1H), 1.87 (dddd, J=13.6, 13.6, 4.2, 3.3 Hz; 1H), 2.00 (ddddd, J=13.0, 13.0, 13.0, 4.3, 4.3 Hz; 1H), 2.20 (m; 1H), 3.51 (ddd, J=11.9, 2.4 Hz; 1H), 3.74 (m; 1H), 3.80 (ddd, J=6.7, 5.7, 1.8 Hz; 1H), 4.06 (m; 1H), 4.36 (dd, J=11.5, 5.7 Hz; 1H), 4.43 (dd, J=11.5, 6.8 Hz; 1H), 7.44 (dd, J=7.9, 7.4 Hz; 2H), 7.57 (dddd, J=7.4, 7.4, 1.9, 1.4 Hz; 1H), 8.06 ppm (m; 2H); ^{13}C NMR (100 MHz; $CDCl_3$): δ=20.7 (t), 27.3 (t), 56.7 (d), 64.7 (t), 68.1 (t), 76.1 (d), 128.4 (d), 129.7 (d), 129.9 (s), 133.1 (d), 166.3 ppm (s); IR (film, NaCl plates): $\tilde{\nu}$=3064, 2955, 2859, 2104, 1721, 1273, 1092, 952 cm^{-1}; MS (EI): *m/z* (relative intensity): 139 $[M-BzOH]^+$(7), 111 (12), 105 (100); elemental analysis (%) calcd for $C_{13}H_{15}N_3O_3$: C 59.76, H 5.79, N 16.08; found: C 60.09, H 5.91, N 15.69.

tert-Butyl 2-{[(2*S*,3*R*)-3-azidotetrahydro-2*H*-pyran-2-yl]methoxy}acetate (6)

Sodium carbonate (0.32 g, 3.1 mmol) was added to **13** (8.0 g, 30.6 mmol) dissolved in methanol (76 mL, 0.4 M). After stirring for 2 h, the reaction mixture was filtered through celite and washed with methanol (3×10 mL). The solvent was removed under reduced pressure and the crude product was purified by column chromatography to give the expected primary alcohol.

NaH (60% in mineral oil, 1.37 g, 34.4 mmol) was added to a solution of primary alcohol (4.5 g, 28.6 mmol) in THF (50 mL) at 0 °C with stirring for 5 min. A solution of *tert*-butylbromoacetate (8.5 mL, 57.3 mmol) in THF (100 mL) was then added portionwise at 0 °C. The reaction mixture was allowed to warm to room temperature and stirred for 2 h. The reaction mixture was cooled to 0 °C and quenched by the slow addition of water. The reaction mixture was extracted with EtOAc (3×50 mL), the organic layer was dried over $MgSO_4$, the solvent was removed under reduced pressure, and the crude product was purified by column chromatography to give **6** (6.2 g, 75% yield) as an oil. $[\alpha]_D^{25}=-55.3$ (c=1.6 in $CHCl_3$); ^{1}H NMR (400 MHz; $CDCl_3$): δ=1.44 (m; 1H), 1.46 (s; 9H), 1.80 (dddd, J=13.6, 13.6, 3.7, 3.7 Hz; 1H), 1.94 (ddddd, J=13.6, 13.4, 13.1, 4.4, 4.4 Hz; 1H), 2.14 (d, J=16.2 Hz; 1H), 3.48 (ddd, J=11.9, 11.9, 2.4 Hz; 1H), 3.58 (d, J=1.9 Hz; 1H), 3.60 (s; 1H), 3.67 (m; 1H), 3.70 (m; 1H), 3.96 (d, J=16.3 Hz; 1H), 4.01 (m; 1H), 4.02 ppm (d, J=16.3 Hz; 1H); ^{13}C NMR (100 MHz; $CDCl_3$): δ=20.7 (s), 27.3 (s), 28.1 (t), 56.7 (s), 68.2 (s), 69.2 (s), 71. 6 (s), 77.0 (t), 77.3 (s), 81.7 (s) 169.4 ppm (s); IR (CH_2Cl_2): $\tilde{\nu}$=3026, 3011, 2982, 2933, 2859, 2105, 1742, 1370, 1148 cm^{-1}; HRMS (ESI): *m/z*: calcd for $C_{12}H_{21}N_3O_4Na$ $[M+Na]^+$: 294.1430; found: 294.1434.

Dipeptide(OMe) (16)

Compound **5** was separated into two portions. One portion was used to convert the *tert*-butyl ester moiety into the carboxylic acid group under the following conditions:

General procedure for the deprotection of the *tert*-butyl ester

Trifluoroacetic acid (2 mL) was added to a solution of **5** (1.9 g, 6.3 mmol) in CH_2Cl_2 (10 mL) with stirring for 2 h (monitored by TLC analysis) at room temperature. The solvent and trifluoroacetic acid were removed under reduced pressure, and the expected carboxylic acid **14** was used without purification.

The second portion was used to convert the azide group into the amine group under the following conditions:

General procedure for the reduction of the azide

Compound **5** (1.9 g, 6.3 mmol) was added to a suspension of 5 wt% Pd/C (catalytic) in methanol (50 mL) with stirring for 1–3 h (monitored by TLC analysis) at room temperature under 1 atm of H_2 pressure. The reaction mixture was filtered through celite and washed with methanol (3×25 mL). The filtrate was collected and the solvents were removed by rotary evaporation, thus affording the expected amine **15**, which was used without purification.

General coupling procedure

The corresponding carboxylic acid **14** and amine **15** were dissolved in CH_2Cl_2 (60 mL). DIPEA (2.2 mL, 12.6 mmol), HOBt (1.7 g, 12.6 mmol), and EDCI (2.4 g, 12.6 mmol) were added to the reaction mixture, which was stirred overnight. The reaction mixture was quenched with water and extracted with CH_2Cl_2 (3×20 mL). The organic layer was dried over $MgSO_4$, filtered, concentrated, and the crude product was purified by column chromatography to give **16** (2.2 g, 70% yield) as an oil. $[\alpha]_D^{25}=+3.1$ (c=1.3 in $CHCl_3$); ^{1}H NMR (400 MHz; $CDCl_3$): δ=1.45 (s; 9H), 1.62 (dddd, J=12.3, 12.3, 12.3, 5.1 Hz; 1H), 1.80 (m; 2H), 1.96 (dddd, J=12.6, 12.6, 12.6, 4.9 Hz; 1H), 3.38 (s; 3H), 3.41 (m; 1H), 3.44 (s; 3H), 3.51 (m; 3H), 3.63 (m; 6H), 3.87 (m; 1H), 4.01 (m; 6H), 4.57 (dd, J=10.3, 3.4 Hz; 1H), 6.89 ppm (d, J=10.3 Hz; 1H); ^{13}C NMR (100 MHz; $CDCl_3$): δ=26.9 (t), 28.1 (t), 28.1 (q), 45.8 (d), 55.8 (q), 56.2 (q), 58.8 (d), 66.0 (t), 66.3 (t), 69.1 (t), 71.0 (t), 72.0 (t), 72.2 (t), 76.2 (d), 77.3 (d), 77.7 (d), 79.4 (d), 81.6 (s), 169.5 (s), 169.8 ppm (s); IR (film, NaCl plates): $\tilde{\nu}$=3416, 3338, 2947, 2858, 2104, 1747, 1677, 1098 cm^{-1}; HRMS (ESI): *m/z*: calcd for $C_{22}H_{38}N_4O_9Na$ $[M+Na]^+$: 525.2536; found: 525.2556.

Cyclodipeptide(OMe) (1): The general procedure for reduction of azide was applied to **16** (110 mg, 0.22 mmol) to afford the expected amine, which was used without purification.

Then, the general procedure to deprotect the *tert*-butyl ester moiety was applied to the amine obtained above to obtain the expected amino acid **26**, which was used without purification.

General cyclization procedure: The corresponding amino acid **26** was dissolved in CH_2Cl_2 (110 mL). DIPEA (0.06 mL, 0.34 mmol), HOBt (46 mg, 0.34 mmol), and EDCI (66 mg, 0.34 mmol) were added to the mixture, which was stirred for 5 days. The reaction mixture was quenched with water and extracted with CH_2Cl_2 (3×20 mL). The organic layer was dried over $MgSO_4$, filtered, concen-

trated, and the crude product was purified by column chromatography to give **1** (34 mg, 38% yield) as an oil. $[\alpha]_D^{25} = +5.9$ ($c = 1.2$ in $CDCl_3$); ^1H NMR (500 MHz; $CDCl_3$): $\delta = 1.74$ (dddd, $J = 13.2$, 13.2, 11.8, 5.3 Hz; 2H), 1.87 (m; 2H), 3.34 (s; 6H), 3.39 (dd, $J = 10.7$, 10.3 Hz; 2H), 3.47 (ddd, $J = 11.7$, 4.9, 3.9 Hz; 2H), 3.61 (ddd, $J = 12.7$, 12.6, 2.6 Hz; 2H), 3.69 (ddd, $J = 10.7$, 4.6, 1.0 Hz; 2H), 3.77 (dd, $J = 10.3$, 4.6 Hz; 2H), 3.87 (d, $J = 16.4$ Hz; 2H), 4.11 (ddd, $J = 12.1$, 5.2, 1.2 Hz; 2H), 4.26 (d, $J = 16.4$ Hz; 2H), 4.53 (dd, $J = 10.4$, 3.8 Hz; 2H), 7.65 ppm (d, $J = 10.4$ Hz; 2H); ^{13}C NMR (100 MHz; $CDCl_3$): $\delta =$ 27.72 (t), 45.16 (d), 55.78 (q), 66.85 (t), 69.57 (t), 70.40 (t), 75.76 (d), 76.51 (d), 170.35 ppm (s); IR (CH_2Cl_2): $\tilde{\nu} = 3336$, 2957, 2933, 2866, 1674, 1533, 1266, 1127, 1087, 848 cm^{-1}; HRMS (ESI): *m/z*: calcd for $C_{18}H_{30}N_2O_8Na$ $[M+Na]^+$: 425.1900; found: 425.1898.

Tetrapeptide(OMe) (19): Compound **16** was separated in two portions. One portion was used to convert the *tert*-butyl ester moiety into a carboxylic acid group under the following conditions: The general procedure to deprotect the *tert*-butyl ester moiety was applied to **16** (1 g, 2.0 mmol), and the expected carboxylic acid **17** was used without purification.

The second portion was used to convert the azide group into the amine group under the following conditions: The general procedure for reduction of azide was applied to **16** (1 g, 2.0 mmol) to afford the expected amine **18**, which was used without purification.

The general coupling procedure described above was used with carboxylic acid **17** and amine **18** to give **19** (1.23 g, 68% yield) as an oil. $[\alpha]_D^{25} = +4.9$ ($c = 1.1$ in $CHCl_3$); ^1H NMR (400 MHz; $CDCl_3$): $\delta =$ 1.45 (s; 9H), 1.65 (m; 2H), 1.80 (m; 4H), 1.95 (m; 2H), 3.35 (s; 6H), 3.36 (s; 3H), 3.40 (m; 3H), 3.43 (s; 3H), 3.45 (m; 2H), 3.51 (m; 5H), 3.58 (m; 6H), 3.64 (m; 3H), 3.70 (m; 2H), 3.87 (m; 1H), 3.95 (d, $J =$ 4.1 Hz; 2H), 4.00 (d, $J = 3.4$ Hz; 2H), 4.05 (m; 7H), 4.54 (m; 3H), 6.83 (d, $J = 10.2$ Hz; 1H), 6.85 (d, $J = 9.8$ Hz; 1H), 6.86 ppm (d, $J =$ 10.3 Hz; 1H); ^{13}C NMR (100 MHz; $CDCl_3$): $\delta = 26.9$ (t), 27.9 (t), 28.0 (t), 28.1 (q), 45.6 (q), 45.7 (q), 45.8 (q), 55.8 (d), 56.0 (d), 56.1 (d), 56.1 (d), 58.8 (d), 66.0 (t), 66.1 (t), 66.2 (t), 66.3 (t), 69.1 (t), 70.9 (t), 71.0 (t), 72.1 (t), 72.2 (t), 72.3 (t), 76.3 (d), 76.9 (d), 77.0 (d), 77.2 (d), 77.6 (d), 77.8 (d), 79.4 (d), 81.6 (s), 169.4 (s), 169.8 (s), 169.9 (s), 170.0 ppm (s); IR (film, NaCl plates): $\tilde{\nu} = 3416$, 2985, 2929, 2107, 1682, 1048 cm^{-1}; HRMS (ESI): *m/z*: calcd for $C_{40}H_{68}N_6O_{17}Na$ $[M+Na]^+$: 927.4539; found: 927.4516.

Cyclotetrapeptide(OMe) (3): The general procedure for reduction of azide was applied to **19** (140 mg, 0.156 mmol) to afford the expected amine, which was used without purification.

Then the general procedure to deprotect the *tert*-butyl ester moiety was applied to the amine obtained above to provide the expected amino acid **27**, which was used without purification.

The general cyclization procedure described above was applied to the corresponding amino acid **27** to give **3** (54 mg, 43% yield) as an oil. $[\alpha]_D^{25} = +6.1$ ($c = 1.3$ in $CHCl_3$); ^1H NMR (500 MHz; C_6D_6): $\delta =$ 1.39 (dd, $J = 13.0$, 4.2 Hz; 4H), 1.67 (dddd, $J = 13.0$, 12.9, 12.6, 5.1 Hz; 4H), 2.89 (ddd, $J = 11.9$, 4.5, 4.3 Hz; 4H), 3.03 (ddd, $J = 12.9$, 11.7, 2.4 Hz; 4H), 3.20 (ddd, $J = 8.5$, 2.4, 1.6 Hz; 4H), 3.22 (s; 12H), 3.51 (dd, $J = 11.0$, 2.5 Hz; 4H), 3.61 (dd, $J = 11.0$, 8.5 Hz; 4H), 3.70 (dd, $J = 11.7$, 4.1 Hz; 4H), 3.88 (d, $J = 15.8$ Hz; 4H), 4.05 (d, $J =$ 15.8 Hz; 4H), 4.50 (dd, $J = 10.0$, 4.0 Hz; 4H), 7.22 ppm (d, $J =$ 10.1 Hz; 4H); ^{13}C NMR (100 MHz; C_6D_6): $\delta = 27.9$ (t), 45.3 (d), 55.4 (q), 65.9 (t), 70.1 (t), 72.9 (t), 76.6 (d), 77.2 (d), 169.7 ppm (s); IR (CH_2Cl_2, 7 mM): $\tilde{\nu} = 3414$, 3388, 3350, 2930, 2862, 1678, 1527, 1089, 848 cm^{-1}; HRMS (ESI): *m/z*: calcd for $C_{36}H_{60}N_4O_{16}Na$ $[M+Na]^+$: 827.3902; found: 827.3873

Dipeptide (22): Compound **6** was separated in two portions. One portion was used to convert the *tert*-butyl ester moiety into a carboxylic acid group under was applied to the following conditions: The general procedure to deprotect the *tert*-butyl ester moiety was applied to **6** (2.0 g, 7.4 mmol) to obtain the expected carboxylic acid **20**, which was used without purification.

The second portion was used to convert the azide group into the amine group under the following conditions: The general procedure for reduction of azide was applied to **6** (2.0 g, 7.4 mmol) to afford the expected amine **21**, which was used without purification.

The general coupling procedure described above was used with carboxylic acid **20** and amine **21** to give **22** (2.2 g, 68% yield) as an oil. $[\alpha]_D^{25} = -39.1$ ($c = 1.4$ in $CHCl_3$); ^1H NMR (400 MHz; $CDCl_3$): $\delta =$ 1.40 (s; 9H), 1.64–1.92 (m; 7H), 2.18 (d, $J = 13.6$ Hz; 1H), 3.45–3.65 (m; 8H), 3.75 (m; 1H), 3.92–4.15 (m; 7H), 7.33 ppm (d, $J = 8.8$ Hz; 1H); ^{13}C NMR (75 MHz; $CDCl_3$): $\delta = 20.7$ (t), 20.9 (t), 27.2 (t), 28.1 (q), 28.6 (t), 44.7 (d), 56.5 (d), 67.9 (t), 68.6 (t), 69.1 (t), 70.8 (t), 72.2 (t), 72.4 (t), 76.8 (d), 78.3 (d), 81.4 (s), 169.2 (s), 169.4 ppm (s); IR (film, NaCl plates): $\tilde{\nu} = 3416$, 3338, 3059, 2948, 2859, 2104, 1748, 1677, 1529, 1098 cm^{-1}; HRMS (ESI): *m/z*: calcd for $C_{20}H_{34}N_4O_7Na$ $[M+Na]^+$: 465.2325; found: 465.2329.

Cyclodipeptide (2): The general procedure for reduction of the azide moiety was applied to **22** (140 mg, 0.32 mmol) to afford the expected amine, which was used without purification.

Then, the general procedure to deprotect the *tert*-butyl ester moiety was applied to the amine obtained above to give the expected amino acid **28**, which was used without purification.

The corresponding amino acid **28** was dissolved in CH_2Cl_2 (64 mL). DIPEA (0.164 mL, 0.96 mmol) and HBTU (146 mg, 0.38 mmol) were added to the reaction mixture, which was stirred for 5 days. The reaction mixture was quenched with water and extracted with CH_2Cl_2 (3×20 mL). The organic layer was dried over $MgSO_4$, filtered, concentrated, and the crude product was purified by column chromatography to give **2** (34 mg, 31% yield) as an oil. $[\alpha]_D^{25} = +67.6$ ($c = 1.5$ in $CHCl_3$); ^1H NMR (500 MHz; C_6D_6): $\delta = 0.82$ (bdd, $J = 13.7$, 2.0 Hz; 2H), 1.19 (dddd, $J = 13.5$, 13.5, 3.5, 3.5 Hz; 2H), 1.54 (ddddd, $J = 13.7$, 13.5, 12.8, 4.5, 4.5 Hz; 2H), 2.06 (bd, $J = 13.5$ Hz; 2H), 2.92 (ddd, $J = 4.6$, 4.6, 1.5 Hz; 2H), 2.97 (ddd, $J = 12.7$, 11.3, 2.5 Hz; 2H), 2.99 (dd, $J = 10.3$, 5.0 Hz; 2H), 3.33 (dd, $J = 10.3$, 4.0 Hz; 2H), 3.56 (dd, $J = 11.2$, 5.0 Hz; 2H), 3.69 (d, $J = 14.7$ Hz; 2H), 3.88 (d, $J =$ 14.7 Hz; 2H), 3.99 (m; 2H), 7.72 ppm (bd, $J = 7.0$ Hz; 2H); ^{13}C NMR (100 MHz; C_6D_6): $\delta = 20.6$ (t), 28.5 (t), 46.6 (d), 68.9 (t), 71.3 (t), 72.1 (t), 76.5 (d), 168.1 ppm (s); IR (CH_2Cl_2): $\tilde{\nu} = 3425$, 3331, 3186, 3066, 2932, 2859, 1671, 1536, 1265, 1134, 1097, 1070, 848 cm^{-1}; HRMS (ESI): *m/z*: calcd for $C_{16}H_{26}N_2O_6Na$ $[M+Na]^+$: 365.1689; found: 365.1692.

Tetrapeptide (25): Compound **22** was separated into two portions. One portion was used to convert the *tert*-butyl ester moiety into a carboxylic acid group under the following conditions: The general procedure to deprotect the *tert*-butyl ester moiety was applied to **22** (1 g, 2.3 mmol) to obtain the expected carboxylic acid **23**, which was used without purification.

The second portion was used to convert the azide group into an amine group under the following conditions: The general procedure for reduction of the azide moiety was applied to **22** (1 g, 2.3 mmol) to afford the expected amine **24**, which was used without purification.

The general coupling procedure described above was used with the corresponding carboxylic acid **23** and amine **24** to give **25** (1.1 g, 62% yield) as an oil. $[\alpha]_D^{25} = -12.3$ ($c = 1.3$ in $CHCl_3$); ^1H NMR (400 MHz; $CDCl_3$): $\delta = 1.45$ (s; 9H), 1.48 (m; 4H), 1.75 (m; 6H), 1.90 (m; 5H), 2.18 (d, $J = 13.7$ Hz; 1H), 3.44–3.77 (m; 17H), 3.90–4.20 (m; 15H), 7.14 (d, $J = 9.3$ Hz; 1H), 7.18 (d, $J = 9.1$ Hz; 1H), 7.29 ppm (d,

$J = 8.7$ Hz; 1H); ^{13}C NMR (100 MHz; $CDCl_3$): $\delta = 20.7$ (t), 20.8 (t), 20.9 (t), 27.2 (t), 28.1 (q), 28.5 (t), 28.6 (t), 44.1 (d), 44.2 (d), 44.4 (d), 56.5 (d), 67.9 (t), 68.5 (t), 68.6 (t), 69.0 (t), 70.7 (t), 70.9 (t), 72.4 (t), 72.4 (t), 72.5 (t), 73.0 (t), 76.8 (d), 78.0 (d), 78.4 (d), 81.5 (s), 169.2 (s), 169.2 (s), 169.4 ppm (s); IR (film, NaCl plates): $\tilde{\nu} = 3413$, 3338, 2944, 2859, 2104, 1746, 1677, 1525, 1099 cm^{-1}; HRMS (ESI): *m/z*: calcd for $C_{36}H_{60}N_6O_{13}Na$ $[M+Na]^+$: 807.4116; found: 807.4137.

Acknowledgements

This research was supported by the Spanish MINECO and cofinanced by the European Regional Development Fund (ERDF) (CTQ2011–22653). A.F.-V. and J.B.G. thank the Spanish MEC for an FPU fellowship.

Keywords: conformation analysis · cyclic peptides · noncovalent interactions · solid-state structures · sugar amino acids

[1] a) E. M. Driggers, S. P. Hale, J. Lee, N. K. Terrett, *Nat. Rev. Drug Discovery* **2008**, *7*, 608–624; b) E. Marsault, M. L. Peterson, *J. Med. Chem.* **2011**, *54*, 1961–2004; c) J. Mallinson, I. Collins, *Future Med. Chem.* **2012**, *4*, 1409–1438; d) A. R. Bogdan, S. V. Jerome, K. N. Houk, K. James, *J. Am. Chem. Soc.* **2012**, *134*, 2127–2138.

[2] D. F. Veber, S. R. Johnson, H.-Y. Cheng, B. R. Smith, K. W. Ward, K. D. Kopple, *J. Med. Chem.* **2002**, *45*, 2615–2623.

[3] J. F. Tjia, I. R. Webber, D. J. Back, *Br. J. Clin. Pharmacol.* **1991**, *31*, 344–346.

[4] A. M. Dahlem, A. S. Hassan, S. P. Swanson, W. W. Carmichael, V. R. Beasley, *Pharmacol. Toxicol.* **1989**, *64*, 177–181.

[5] E. Biron, J. Chatterjee, O. Ovadia, D. Langenegger, J. Brueggen, D. Hoyer, H. A. Schmid, R. Jelinek, C. Gilon, A. Hoffman, H. Kessler, *Angew. Chem.* **2008**, *120*, 2633–2637; *Angew. Chem. Int. Ed.* **2008**, *47*, 2595–2599.

[6] C. A. Lipinski, F. Lombardo, B. W. Dominy, P. J. Feeney, *Adv. Drug Delivery Rev.* **2001**, *46*, 3–26.

[7] a) S. Gangwar, S. D. S. Jois, T. J. Siahaan, D. G. Vander Velde, V. J. Stella, R. T. Borchardt, *Pharm. Res.* **1996**, *13*, 1657–1662; b) T. Rezai, B. Yu, G. L. Millhauser, M. P. Jacobson, R. S. Lokey, *J. Am. Chem. Soc.* **2006**, *128*, 2510–2511; c) T. Rezai, J. E. Bock, M. V. Zhou, C. Kalyanaraman, R. S. Lokey, M. P. Jacobson, *J. Am. Chem. Soc.* **2006**, *128*, 14073–14080; d) S. B. Rafi, B. R. Hearn, P. Vedantham, M. P. Jacobson, A. R. Renslo, *J. Med. Chem.* **2012**, *55*, 3163–3169; e) J. E. Bock, J. Gavenonis, J. A. Kritzer, *ACS Chem. Biol.* **2013**, *8*, 488–499.

[8] a) J. Chatterjee, C. Gilon, A. Hoffman, H. Kessler, *Acc. Chem. Res.* **2008**, *41*, 1331–1342; b) L. Doedens, F. Opperer, M. Cai, J. G. Beck, M. Dedek, E. Palmer, V. J. Hruby, H. Kessler, *J. Am. Chem. Soc.* **2010**, *132*, 8115–8128; c) T. R. White, C. M. Renzelman, A. C. Rand, T. Rezai, C. M. McEwen, V. M. Gelev, R. A. Turner, R. G. Linington, S. S. F. Leung, A. S. Kalgutkar, J. N. Bauman, Y. Zhang, S. Liras, D. A. Price, A. M. Mathiowetz, M. P. Jacobson, R. S. Lokey, *Nat. Chem. Biol.* **2011**, *7*, 810–817; d) J. G. Beck, J. Chatterjee, B. Laufer, M. U. Kiran, A. O. Frank, S. Neubauer, O. Ovadia, S. Greenberg, C. Gilon, A. Hoffman, H. Kessler, *J. Am. Chem. Soc.* **2012**, *134*, 12125–12133; e) J. Chatterjee, F. Rechenmacher, H. Kessler, *Angew. Chem.* **2013**, *125*, 268–283; *Angew. Chem. Int. Ed.* **2013**, *52*, 254–269.

[9] T. K. Chakraborty, S. Jayaprakash, P. V. Diwan, R. Nagaraj, S. R. B. Jampani, A. C. Kunwar, *J. Am. Chem. Soc.* **1998**, *120*, 12962–12963.

[10] E. G. von Roedern, H. Kessler, *Angew. Chem.* **1994**, *106*, 684–686; *Angew. Chem. Int. Ed.* **1994**, *33*, 687–689.

[11] a) E. Locardi, M. Stöckle, S. Gruner, H. Kessler, *J. Am. Chem. Soc.* **2001**, *123*, 8189–8196; b) J. E. Campbell, E. E. Englund, S. D. Burke, *Org. Lett.* **2002**, *4*, 2273–2275; c) M. Stöckle, G. Voll, R. Günther, E. Lohof, E. Locardi, S. Gruner, H. Kessler, *Org. Lett.* **2002**, *4*, 2501–2504; d) T. K. Chakraborty, P. Srinivasu, E. Bikshapathy, R. Nagaraj, M. Vairamani, S. K. Kumar, A. C. Kunwar, *J. Org. Chem.* **2003**, *68*, 6257–6263; e) R. M. van Well, L. Marinelli, C. Altona, K. Erkelens, G. Siegal, M. van Raaij, A. L. Llamas-Saiz, H. Kessler, E. Novellino, A. Lavecchia, J. H. van Boom, M. Overhand, *J. Am. Chem. Soc.* **2003**, *125*, 10822–10829; f) T. K. Chakraborty, D. Koley, S. Prabhakar, R. Ravi, A. C. Kunwar, *Tetrahedron* **2005**, *61*, 9506–9512; g) B. Jagannadh, M. S. Reddy, C. L. Rao, A. Prabhakar, B. Jagadeesh, S. Chandrasekhar, *Chem. Commun.* **2006**, 4847–4849; h) T. K. Chakraborty, S. Roy, D. Koley, S. K. Dutta, A. C. Kunwar, *J. Org. Chem.* **2006**, *71*, 6240–6243; i) F. Fujimura, T. Hirata, T. Morita, S. Kimura, Y. Horikawa, J. Sugiyama, *Biomacromolecules* **2006**, *7*, 2394–2400; j) T. Hirata, F. Fujimura, Y. Horikawa, J. Sugiyama, T. Morita, S. Kimura, *Biopolymers* **2007**, *88*, 150–156; k) F. Fujimura, Y. Horikawa, T. Morita, J. Sugiyama, S. Kimura, *Biomacromolecules* **2007**, *8*, 611–616; l) S. Chandrasekhar, B. Saritha, P. Naresh, M. Udayakiran, C. R. Reddy, B. Jagadeesh, *Helv. Chim. Acta* **2008**, *91*, 1267–1276.

[12] a) R. Carrillo, V. S. Martín, T. Martín, *Tetrahedron Lett.* **2004**, *45*, 5215–5219; b) R. Carrillo, V. S. Martín, M. López, T. Martín, *Tetrahedron* **2005**, *61*, 8177–8191; c) R. Carrillo, M. López-Rodríguez, V. S. Martín, T. Martín, *Angew. Chem.* **2009**, *121*, 7943–7948; *Angew. Chem. Int. Ed.* **2009**, *48*, 7803–7808; d) R. Carrillo, A. Feher-Voelger, T. Martín, *Angew. Chem.* **2011**, *123*, 10804–10808; *Angew. Chem. Int. Ed.* **2011**, *50*, 10616–10620; e) R. Carrillo, E. Q. Morales, V. S. Martín, T. Martín, *Chem. Eur. J.* **2013**, *19*, 7042–7048; f) R. Carrillo, E. Q. Morales, V. S. Martín, T. Martín, *J. Org. Chem.* **2013**, *78*, 7785–7795.

[13] R. Carrillo, M. López-Rodríguez, V. S. Martín, T. Martín, *CrystEngComm* **2010**, *12*, 3676–3683.

[14] a) R. M. van Well, L. Marinelli, K. Erkelens, G. A. van der Marel, A. Lavecchia, H. S. Overkleeft, J. H. van Boom, H. Kessler, M. Overhand, *Eur. J. Org. Chem.* **2003**, 2303–2313; b) M. Ménand, J.-C. Blais, L. Hamon, J.-M. Valéry, J. Xie, *J. Org. Chem.* **2005**, *70*, 4423–4430.

[15] a) I. A. Motorina, C. Huel, E. Quiniou, J. Mispelter, E. Adjadj, D. S. Grierson, *J. Am. Chem. Soc.* **2001**, *123*, 8–17; b) H.-D. Arndt, A. Knoll, U. Koert, *Angew. Chem.* **2001**, *113*, 2137–2140; *Angew. Chem. Int. Ed.* **2001**, *40*, 2076–2078; c) J. T. Ernst, J. Becerril, H. S. Park, H. Yin, A. D. Hamilton, *Angew. Chem.* **2003**, *115*, 553–557; *Angew. Chem. Int. Ed.* **2003**, *42*, 535–539; d) H.-D. Arndt, B. Ziemer, U. Koert, *Org. Lett.* **2004**, *6*, 3269–3272; e) J. P. Saludes, J. B. Ames, J. Gervay-Hague, *J. Am. Chem. Soc.* **2009**, *131*, 5495–5505; f) W. Hu, Q. Yan, D. Zhao, *Chem. Eur. J.* **2011**, *17*, 7087–7094; g) G. V. M. Sharma, K. S. Reddy, S. J. Basha, K. R. Reddy, A. V. S. Sarma, *Org. Biomol. Chem.* **2011**, *9*, 8102–8111; h) G. V. M. Sharma, P. S. Reddy, D. Chatterjee, A. C. Kunwar, *Tetrahedron* **2012**, *68*, 4390–4398.

[16] M. Kanai, Y. Hamashima, M. Shibasaki, *Tetrahedron Lett.* **2000**, *41*, 2405–2409.

[17] G. Snatzke, Z. Raza, I. Habus, V. Sunjic, *Carbohydr. Res.* **1988**, *182*, 179–196.

[18] R. M. Giuliano Jr., A. D. Jordan, A. D. Gauthier, K. Hoogsteen, *J. Org. Chem* **1993**, *58*, 4979–4988.

[19] C.-R. Shie, Z.-H. Tzeng, S. S. Kulkarni, B.-J. Uang, C.-Y. Hsu, S.-C. Hung, *Angew. Chem.* **2005**, *117*, 1693–1696; *Angew. Chem. Int. Ed.* **2005**, *44*, 1665–1668.

[20] In early experiments, the methyl ester unit was employed as the carboxyl protecting group, but the alkoxy group of the starting material reacted with the final product, thus leading to transesterification; the *tert*-butyl ester moiety proved to be hindered enough to effectively prevent this deleterious side reaction.

[21] B. Lal, B. N. Pramanik, M. S. Manhas, A. K. Bose, *Tetrahedron Lett.* **1977**, *18*, 1977–1980.

[22] We also tried a nucleophilic substitution of different sulfonate groups of alcohol **11** (i.e., mesylate and nonaflate) with sodium azide; however, an elimination product was also obtained, albeit in a smaller proportion (the ratio of azide **6**/elimination product was 3.9:1 for the mesylate derivative).

[23] C. Thibaudeau, R. Stenutz, B. Hertz, T. Klepach, S. Zhao, Q. Wu, I. Carmichael, A. S. Serianni, *J. Am. Chem. Soc.* **2004**, *126*, 15668—15685; equations: 1) $2.8P_{gg} + 2.2P_{gt} + 11.1P_{tg} = {}^3J_{C2H,C7HproS}$; 2) $0.9P_{gg} + 10.8P_{gt} + 4.7P_{tg} = {}^3J_{C2H,C7HproR}$; 3) $P_{gg} + P_{gt} + P_{tg} = 1$.

[24] See the Supporting Information.

[25] Crystals of cyclodipeptides **1** and **2** were grown under identical conditions, that is, from a solution of the cyclopeptide in dichloromethane by vapor-phase equilibration with *n*-hexane.

[26] The structure of cyclodipeptides **1** and **2** in the solid state is not completely symmetrical; therefore, it is more appropriate to give an average of the dihedral angles.

[27] CCDC-949309 and -949308 (**1** and **2**, respectively) contains the supplementary crystallographic data for this paper. These data can be obtained free of charge from The Cambridge Crystallographic Data Centre via www.ccdc.cam.ac.uk/data_request/cif.
[28] Chloroform is usually considered as a model for a lipophilic medium, such as the cellular membrane.
[29] Similar values were previously reported, see: R. Vanderesse, V. Grand, D. Limal, A. Vicherat, M. Marraud, C. Didierjean, A. Aubry, *J. Am. Chem. Soc.* **1998**, *120*, 9444 – 9451.
[30] The 2-methoxy group in the acetamide represents the oxygen atom at C7 of the adjacent residue.
[31] S. H. Gellman, G. P. Dado, G.-B. Liang, B. R. Adam, *J. Am. Chem. Soc.* **1991**, *113*, 1164 – 1173.
[32] I. Kolossváry, W. C. Guida, *J. Am. Chem. Soc.* **1996**, *118*, 5011 – 5019.
[33] Maestro, Version 9.3 Schroëdinger, LLC, New York, NY, **2012**.
[34] MacroModel, Version 9.9 Schroëdinger, LLC, New York, NY, **2012**.
[35] G. A. Kaminski, R. A. Friesner, J. Tirado-Rives, W. L. Jorgensen, *J. Phys. Chem. B* **2001**, *105*, 6474 – 6487.
[36] W. L. F. Armarego, D. D. Perrin, *Purification of Laboratory Chemicals*, 4th ed., Butterworth-Heinemann, Oxford, **1996**.

Received: October 1, 2013
Revised: December 16, 2013
Published online on February 25, 2014